GASEOUS AND SURFACE DIFFUSION IN ACTIVATED CARBON

by

THOMAS J. KELLY

Bachelor of Science

University of Notre Dame

South Bend, Indiana

1966

Submitted to the Faculty of the Graduate College
of the Oklahoma State University
in partial fulfillment of the requirements
for the degree of
MASTER OF SCIENCE
May, 1968

GASEOUS AND SURFACE DIFFUSION IN ACTIVATED CARBON

Thesis Approved:

K C Chao
Thesis Adviser

Bd Cypress

N Durham
Dean of the Graduate College

PREFACE

Fluxes of counterdiffusing binary gas mixtures in activated carbon were experimentally measured at constant pressures over the range of 58 to 718 m.m. mercury at approximately 25° C. The data were analyzed by considering the fluxes to be composed of gaseous and surface fluxes in parallel. A bidisperse pore model was used to describe the carbon. Surface diffusivities of propane on activated carbon were evaluated using several methods.

The author wishes to express his appreciation to Dr. K. C. Chao for his assistance and guidance during this study, to Howard Denenholz, who built the apparatus and used it in a previous study, for his helpful suggestions, and to Dr. C. Barrere for his advice on gas chromatography. A special thanks is due Margaret Clark for her patience in organizing and typing the manuscript.

The author is thankful for the financial assistance extended to him during the 1966-67 school year by the National Science Foundation.

TABLE OF CONTENTS

LIST OF TABLES

LIST OF FIGURES

CHAPTER I

INTRODUCTION

Porous pellets have long been used in industrial processes as a means of obtaining a large available surface area within a small volume. Porous pellets are found to be especially suited to adsorption and catalytic reaction processes which require a great deal of surface of a specific nature.

Mass transfer within the pellet may seriously limit the amount of surface which is used effectively. In a study by Denenholz on binary counterdiffusion of hydrocarbons through activated carbon, it was found that gas phase diffusion models alone could not explain the observed fluxes and that occurrence of surface diffusion is indicated. The object of this work is to measure the amount of mass transfer which occurs in the adsorbed phase on the surface of the carbon and to calculate surface diffusivities.

CHAPTER II

MASS TRANSFER IN POROUS SOLIDS

There are three paths of diffusion within a porous adsorbent. First is diffusion in the gas in the pores, second is diffusion in the layer of adsorbed gases on the pellet surface, and third is diffusion in the solid pellet material. Diffusion in the solid pellet material is much slower than in the other two paths and can be safely neglected.

Diffusion of Gases in a Capillary Pore

There are two resistances which control gas phase diffusion within a capillary pore. The first resistance is due to gas molecules colliding with each other and is expressed mathematically for a two-component gas by Fick's Law

$$N_A - X_A (N_A + N_B) = -C D_{AB} \frac{d X_A}{d L} \qquad (1)$$

N_A and N_B are fluxes, X_A is the molar concentration of A in the gas phase, C is the molar density of the gas mixture, L is the length of the pellet in the direction of flux, and D_{AB} is the Fick's Law diffusion coefficient of A and B. It can be shown that $D_{AB} = D_{BA}$ (11). Other symbols are defined in the nomenclature.

The second resistance is due to gas molecules colliding with the walls of the pore and is expressed by Knudsen's Equation

$$N_A = -C\, D_{KA}\, \frac{d\, X_A}{d\, L} \tag{2}$$

D_{KA} is the Knudsen diffusion coefficient and is not dependent on other gases that are present. This coefficient can be estimated by

$$D_{KA} = K_o\, \bar{r}\, \bar{v}_A \tag{3}$$

$$\bar{v}_A = (8\, RT/\pi\, M_A)^{1/2} \tag{4}$$

where $\bar{r}$ is the mean free path, $\bar{v}_A$ is average velocity of the molecules, and K_o is a coefficient which is 2/3 for elastic collisions with the wall and 6/13 for inelastic collisions (11) and (21).

When the mean free path of the molecules is much larger than the dimension of the pores, collision with the walls is the controlling resistance and the gas is said to be in the Knudsen diffusion region. When the mean free path is much smaller than the pore dimension, the gas is said to be in the bulk diffusion region. The range in between the two limiting cases is called the transition region.

Based upon momentum balance considerations, Rothfeld (46), Scott and Dullien (49), and Evans et al. (22) have derived an effective diffusion coefficient D_E valid for the transition region

$$N_A = -C\, D_E\, \frac{d\, X_A}{d\, L} \tag{5}$$

$$D_E = \frac{1}{(1 - \alpha X_A)/D_{AB} + 1/D_{KA}} \tag{6}$$

where

$$\alpha = 1 + N_B/N_A \tag{7}$$

It was first suggested by Hoogschagen (33) and later proved by Evans et al. (22) and Scott and Dullien (49) that the theoretical flux ratio in all three regions is

$$\frac{N_B}{N_A} = -\left[\frac{M_A}{M_B}\right]^{1/2} = \alpha - 1 \tag{8}$$

Models for Porous Pellets

Various physical models of pellets have been proposed for predicting gaseous diffusion through porous media. All of them depend on assumptions as to the physical geometry and interconnection of the pores. Two pore models are described below and equations to predict isothermal, isobaric diffusion rates are listed.

The simplest physical model assumes the porous medium has parallel pores, of uniform size, which follow a tortuous path through the pellet. Rothfeld (11) and others (49, 22) have used the parallel pore model, using Equations (5) and (6) to predict flux within the pores.

They substitute effective bulk and Knudsen diffusion coefficients for the true coefficients into the equations for a single capillary.

$$(D_{AB})_{EFF} = \left(\frac{E}{q_D}\right) D_{AB} \tag{9}$$

$$(D_{KA})_{EFF} = \left(\frac{E}{q_K}\right) D_{KA} \qquad (10)$$

E is the porosity of the pellet and q_D and q_K are bulk and Knudsen tortuosity factors.

The resulting differential equation for flux within a porous pellet is

$$N_A = -C \frac{1}{(1 - \alpha X_A)/(D_{AB})_{EFF} + 1/(D_{KA})_{EFF}} \frac{d X_A}{d L} \qquad (11)$$

Integrating Equation (11) across a pellet of length L

$$N_A = C(D_{AB})_{EFF} \text{ Ln } \frac{1 - X_{AL} + (D_{AB})_{EFF}/(D_{KA})_{EFF}}{1 - X_{AO} + (D_{AB})_{EFF}/(D_{KA})_{EFF}} \qquad (12)$$

A more complex physical model depicts two distinct pore systems within the pellet, a macropore region and a micropore region. Wakao and Smith (54, 55) have used the bidisperse model for pellets prepared by compressing particles of catalyst powder, which themselves are porous. The resulting pellet has micropores within the powder particles and macropore space between the powder particles.

The area void fractions, E_a and E_i, are assumed to be the same as the volume void fractions. When the bidisperse model is cut at a plane perpendicular to the direction of diffusion, and the two surfaces are rejoined, there results three parallel paths for diffusion:

(1) through the macropores with an average area of E_a^2,

(2) through the particles with an average area $(1 - E_a^2)$ and an effective void area of micropores per unit of particle area of $E_i^2/(1 - E_a)^2$;

(3) through the macropores and micropores in series. The average area for this path is $2 E_a(1 - E_a)$.

Figure 1 illustrates this pore distribution.

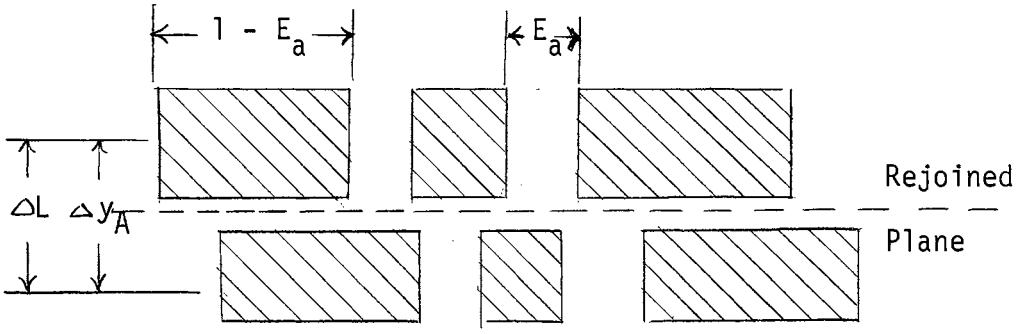

Figure 1. Wakao and Smith Bidisperse Pore Model

Wakao and Smith's equation for the diffusion flux per unit cross sectional area of pellet is

$$N_A = -C\,E_a^{\,2}\,D_a\,\frac{d\,X_A}{d\,L} \quad -C\,(1-E_a)^2\,D_i\,\frac{d\,X_A}{d\,L} \qquad (13)$$

(Macropores) (Micropores)

$$-2\,C\,E_a(1-E_a)\,\frac{2}{(1/D_a)+(1/D_i)}\,\frac{d\,X_A}{d\,L}$$

(Macro- and Micropores in Series)

where

$$D_a = \frac{1}{(1-\alpha X_A)/D_{AB} + (1/D_{KA_a})} \qquad (14)$$

$$D_i = \frac{E_i^{\,2}\,/\,(1-E_a)^2}{(1-\alpha X_A)/D_{AB} + (1/D_{KA_i})} \qquad (15)$$

D_{KA_a} and D_{KA_i} are the Knudsen diffusivities for component A in the macro- and micropore regions.

Substituting Equations (14) and (15) into Equation (13) and integrating across a pellet of length L

$$N_A \frac{L \alpha}{C D_{AB}} = E_a^2 \, \mathrm{Ln}\left\{\frac{1 - \alpha X_{AL} + (D_{AB}/D_{KA_i})}{1 - \alpha X_{AO} + (D_{AB}/D_{KA_i})}\right\} \tag{16}$$

$$+ E_i^2 \, \mathrm{Ln}\left\{\frac{1 - \alpha X_{AL} + (D_{AB}/D_{KA_i})}{1 - \alpha X_{AO} + (D_{AB}/D_{KA_i})}\right\}$$

$$+ \frac{4 E_a (1 - E_a)}{1 + (1 - E_a)^2/E_i^2} \, \mathrm{Ln}\left\{\frac{1 - \alpha X_{AL} + \frac{D_{AB}}{D_{KA_i}} (1 - E_a)^2 + (D_{KA_i}/D_{KA_a})}{1 - \alpha X_{AO} + \frac{D_{AB}}{D_{KA_i}} \frac{(1 - E_a)^2/E_i^2 + (D_{KA_i}/D_{KA_a})}{1 + (1 - E_a)^2/E_i^2}}\right\}$$

A shortened form of Equation (16) is obtained by Wakao and Smith by assuming $\bar{r}_a \gg \bar{r}_i$, so that D_{KA_i}/D_{KA_a} is small with respect to $(1 - E_a)^2/E_i^2$ and D_{AB}/D_{KA_i} is large enough for the arithmetic mean to approach closely the logarithmic mean.

This simplified equation is

$$N_A \frac{L \alpha}{C D_{AB}} = E_a^2 \, \mathrm{Ln}\left\{\frac{1 - \alpha X_{AL} + (D_{AB}/D_{KA_a})}{1 - \alpha X_{AO} + (D_{AB}/D_{KA_a})}\right\} \tag{17}$$

$$+ E_i^2 \quad \frac{\alpha (X_{AO} - X_{AL})}{1 - \alpha [(X_{AO} + X_{AL})/2] + (D_{AB}/D_{KA_i})}$$

$$+ \frac{4 E_a (1 - E_a)}{1 + [(1 - E_a)^2/E_i^2]} \quad \frac{\alpha (X_{AO} - X_{AL})}{1 - \alpha [(X_{AO} + X_{AL})/2] + \left(\dfrac{D_{AB}/D_{KA_i}}{1 + \dfrac{E_i^2}{(1 - E_a)^2}}\right)}$$

Diffusion in the Adsorbed Phase

The second major path for diffusion in porous pellets is in the molecules adsorbed on the walls of the pores. An excellent review of the theory of surface diffusion is given by Darcey (18).

Adsorption is conveniently classified as less than a monomolecular coverage of the surface, monolayer coverage, multilayer coverage, and capillary condensation. In capillary condensation the pore diameter is so small that multilayers from the sides meet at the middle, completely filling the pore space with adsorbate.

The distinction between these are not exact, as multilayers may begin to build up in one place before the monolayer is completed.

The adsorption may be localized and occur at specific sites on the surface where the molecule achieves a minimum potential energy, or it may be nonlocalized, and occur at any point on the surface. Localized and nonlocalized adsorption may both allow an adsorbed molecule to move about while on the surface.

At low surface concentration, for nonlocalized adsorption, the molecules have approximately the same energy at any point on the surface, and are free to move about like a two-dimensional gas. A two-dimensional pressure, or spreading pressure (ϕ), exists in the adsorbed phase and may be thought of as the force that must be applied to keep the film from spreading onto clean surface.

At low surface concentration in the case of localized adsorption, the molecules have to possess sufficient energy to pass over an energy barrier between two adsorption sites. Two limiting cases exist for localized diffusion.

First, if this energy barrier is low compared to the average energy of adsorbed molecules, then movement on the surface would be similar to that of nonlocalized adsorption, i.e., as a two-dimensional gas.

Second, the energy barrier between the site is greater than the average energy of the molecules, hence the adsorbed molecules cannot behave like a two-dimensional gas but must move by activated diffusion between adsorption sites. A spreading pressure is still found in the adsorbate. The mechanism of activated diffusion is analogous to Knudsen diffusion where an adsorption site corresponds to the wall and a slip across the surface is equivalent to a free flight between walls.

A diffusion coefficient at low surface concentrations may be defined as

$$N_{SA} = -D_{SA} \frac{d \overline{C}_A}{d L} \tag{18}$$

$$D_{SA} = 1/2 \, \overline{v}_A \, \lambda \tag{19}$$

D_{SA} is the surface diffusivity, $\overline{C}_A$ is the molar density of A on the surface, moles per gram pellet, $\overline{v}_A$ is the average molecular velocity on the surface, and λ is the mean free path for a two-dimensional gas and the distance between unoccupied sites for activated adsorption.

For a two-dimensional gas

$$\overline{v}_A = \sqrt{\frac{R \, T}{2 \, M_A}} \tag{20}$$

For activated adsorption

$$\overline{v}_A = \frac{\lambda}{\tau} \tag{21}$$

τ is the average time between activated jumps of a molecule on the surface.

Both of these basic adsorption models might be required for the same gas. In a solid system at varying conditions, the localized adsorption and activated diffusion model would be more appropriate at low temperatures and the two-dimensional gas model at high temperatures. The transition region would probably require a combination of both

models. Hwang and Kammermeyer (34, 35, 36, 37) have analyzed the dependence of diffusion on temperature as a means of estimating surface diffusivities.

Also, it is sometimes the case that adsorbates which are described well by a two-dimensional gas model at intermediate and high surface coverages may become highly localized at very small coverages.

As the surface concentration increases, the adsorbed molecules cease to behave as a two-dimensional gas and increasingly tend to act as a liquid. In nonlocalized adsorption, condensation to a liquid usually occurs before the monolayer is completed. In localized adsorption, multilayers form in which the upper layers become a liquid-like film. These films are found, however, to be less mobile than bulk liquid.

At higher concentration, hydrodynamic laws best predict the behavior of the adsorbate. The spreading pressure of the adsorbed phase is commonly used with the hydrodynamic correlations predicting surface flux at these concentrations.

Surface Diffusion in Porous Pellets

Several equations have been suggested to correlate and predict surface flux in porous pellets. The same pore models of pellets that were suggested for gaseous diffusion have been used for surface diffusion.

The driving force for surface diffusion has been suggested by some authors to be the concentration of adsorbate per unit surface area of adsorbent and by others to be the spreading pressure (ϕ) of the adsorbate on the surface.

Spreading Pressure Driving Force

Babbitt (3) offered the following equation for flux of adsorbed molecules in porous media

$$\frac{d \phi}{d L} + C_m u = 0 \qquad (22)$$

u is the component of molecular velocity in the direction of flux. He later offered an alternate form of this equation (4, 5)

$$\frac{d \phi}{d L} + C_n \overline{C} u = 0 \qquad (23)$$

C_m and C_n are coefficients of resistance per cc of pellet and per mole adsorbate respectively, and are constant when the respective equations are valid.

Babbitt (18) concluded that the proper equation was dictated by the variation of the heat of adsorption with concentration. Equation (22) assumes that the heat of adsorption varies as $1/\overline{C}$. This is a fair approximation of the actual case in many instances. Equation (23) assumes that the heat of adsorption is independent of concentration, which is seldom the case. Equation (22) is found to be the more useful of the two cases. For cases in which the heat of adsorption varies as some other function of surface concentration, neither coefficient, C_m or C_n, will be constant.

The spreading pressure ϕ is shown to be a function of surface concentration and temperature from statistical thermodynamics. Babbitt uses the relations between ϕ and the surface concentration given by Fowler and Guggenheim (27) for several different types of adsorption isotherms.

(a) Mobile Monolayer (Henry's Law Adsorption)

$$\overline{C} = H\,P \tag{24}$$

$$\phi = \overline{C}\,R\,T \tag{25}$$

where H is the Henry's Law constant.

(b) Ideal Localized Monolayer (Langmuir Adsorption)

$$\overline{C} = \frac{A_m\,b\,P}{1 + b\,P} \tag{26}$$

$$\phi = A_m b\,R\,T\,\mathrm{Ln}\,\frac{1}{(1 - (\overline{C}/A_m))} \tag{27}$$

where A_m and b are constants.

Gilliland et al. (28, 29, 30) obtained a general relation between ϕ and the concentration in the adsorbed layer with the assumption that the ideal gas law is obeyed in the gas phase. They obtained

$$R\,T\,\frac{d\,P}{P} = \frac{1{,}000\,S\,d\,\phi}{\overline{C}} \tag{28}$$

Combining this expression for ϕ, the parallel pore model tortuosity factor and Equation (22), and integrating over a pellet of length L, the expression for surface flux in a pellet at isothermal conditions is given by

$$N_{SA} = \frac{\rho_{app.}\,S\,RT}{q\,C_{RA}\,L} \int_{P_{AL}}^{P_{Ao}} \frac{\overline{C}_A^{\,2}}{P_A}\,d\,P_A \tag{29}$$

This expression permits graphical integration of adsorption data, eliminating the need of fitting an equation to the adsorption isotherm. It is obvious that if such an equation is available, Equation (29) may be integrated directly.

The coefficient of resistance, C_R, in Equation (29) is found by Gilliland et al. (3,4,5) to be a constant for several Hydrocarbons on Vycor glass. Ash, Barrier and Pope (1,2), however, have found that C_R varies with concentration for systems of CO_2, SO_2, and N_2 on active carbon.

No one has yet published a spreading pressure correlation using a bidispersed pore model.

Surface Concentration Driving Force

The general form of diffusion equation used with surface concentration as the driving force is

$$N_A = -D_{SA} \frac{d \bar{C}_A}{d L} \tag{30}$$

The form of this equation indicates an implicit assumption that the surface flux of one component is independent of the rate of flux of other components diffusing.

Using the parallel pore tortuosity factor, the equation for surface flux in a porous pellet is

$$N_{SA} = \frac{\rho_{app.} S}{q} D_{SA} \frac{d \bar{C}_A}{d L} \tag{31}$$

The integration of this equation across a pellet would depend upon the equation used to relate surface concentration, $\bar{C}$, with the partial pressure in the gas phase, p.

A general relation between $\overline{C}$ and the partial pressure, p_A, is

$$\overline{C} = K(p_A) \cdot p_A \tag{32}$$

where $K(p_A)$ may be a function of p_A or may be a constant (i.e., Henry's Law).

The general form of Equation (31) is then

$$N_{SA} = \frac{\rho_{app.}\, S}{q} D_{SA} \frac{d\,(p_A K(p_A))}{d\,L} \tag{33}$$

or

$$N_{SA} = \frac{\rho_{app.}\, S}{q} D_{SA} \left[K(p_A) \frac{d\,p_A}{d\,L} + p_A \frac{\partial\, K(p_A)}{\partial p_A} \frac{d\,p_A}{d\,L} \right] \tag{34}$$

Integrating Equation (34) across a pellet

$$N_{SA} = \frac{\rho_{app.}\, S}{q\,L} \overline{D_{SA}} \int_{p_{AL}}^{p_{Ao}} K(p_A)\, d\,p_A + \int_{p_{AL}}^{p_{Ao}} \frac{K(p_A)}{p_A}\, p_A\, d\,p_A \tag{35}$$

Rivarola and Smith (44) derive an expression for surface flux using the Wakao and Smith bidispersed pore model. The assumption is made that the diffusion process occurs in the linear section of the equilibrium adsorption curve and therefore K(p) is equal to the Henry's Law constant, H.[1]

Their differential equation is

$$N_{SA} = -2\, D_{SA}\, H \left[\frac{E_a^{\,2}}{\overline{r}_a} + \frac{E_i^{\,2}}{\overline{r}_i} \frac{4\, E_a\, (1 - E_i)}{\overline{r}_a} \right] \frac{d\,p_A}{d\,L} \tag{36}$$

---

[1] Rivarola and Smith used $\overline{C}_A = K_S\, C_A$ and assumes the perfect gas law holds. This results in: $H = K_S/RT$.

The integrated form is

$$N_{SA} = 2\,HP\,D_{SA}\left[\frac{E_a^2}{\bar{r}_a} + \frac{E_i^2}{\bar{r}_i} + \frac{4\,E_a\,(1 - E_i)}{\bar{r}_a}\right]\cdot\ \frac{X_{Ao} - X_{AL}}{L} \qquad (37)$$

The equations of Rivarola and Smith can be extended to include adsorption curves other than linear, using the same procedure that was earlier suggested for the parallel pore model. The generalized form of Equation (36) is

$$N_{SA} = -2\,D_S\left[\frac{E_a^2}{\bar{r}_a} + \frac{E_i^2}{\bar{r}_i} + \frac{4\,E_a\,(1 - E_i)}{\bar{r}_a}\right]\cdot \qquad (38)$$

$$\left[K(p_A)\,\frac{d\,p_A}{d\,L} + p\,\frac{\partial\,K(p_A)}{\partial\,p_A}\quad\frac{d\,p_A}{d\,L}\right]$$

Integrating this equation of a pellet of length L, gives

$$N_{SA} = \frac{2\,D_S}{L}\left[\frac{E_a^2}{\bar{r}_a} + \frac{E_i^2}{\bar{r}_i} + \frac{4\,E_a\,(1 - E_i)}{\bar{r}_a}\right]\cdot \qquad (39)$$

$$\left[\int_{p_{AL}}^{p_{Ao}} K(p_A)\,d\,p_A + \int_{p_{AL}}^{p_{Ao}} \frac{\partial\,K(p_A)}{\partial\,p}\;p_A\,d\,p_A\right]$$

Using the Langmuir adsorption model, the equation becomes

$$N_{SA} = \frac{2\,D_S}{L}\left[\frac{E_a^2}{\bar{r}_a} + \frac{E_i^2}{\bar{r}_i} + \frac{4\,E_a(1 - E_a)}{\bar{r}_a}\right]\cdot \qquad (40)$$

$$\frac{A_m(b\,p_{Ao} - b\,p_{AL})}{(1 + b\,p_{Ao})(1 + b\,p_{AL})}$$

CHAPTER III

EXPERIMENTAL INVESTIGATIONS

Equipment

The method of determination of diffusive flux rates used in this experiment is based upon the method first used by Wilke and Kallenback (57). Two inlet gases are steadily blown across opposite faces of a pellet while the outlet gases are drawn out of the system at such a rate as to maintain steady equal pressure on both sides of the pellet. Using the flow rates of the inlet streams and the concentrations of the inlet and outlet streams, the flux rates through the pellet can be determined and the effective diffusivity can be estimated.

The equipment used here consist of three functional modules as shown in Figure 2: flow meters for the pure gas inlet streams, diffusion cell, and composition analyzer for the outlet sreams.

Heavy walled stainless steel capillary tubing is used for the flowmeters. The tubes are 1/8-inch outside diameter and six feet in length with a nominal inside diameter of 1/2 millimeter. Pressure at the high pressure end of the capillary is measured with a 32-inch U-tube manometer made of seven millimeter glass tubing and filled with mercury. The same type of glass tubing is used to make the 36-inch high U-tube filled with technical grade triethylene glycol (T.E.G.) which is used to measure the pressure drop across the capillary. T.E.G. is used because of its low density and extremely low vapor

pressure. The flowmeters are connected to the gas supply tanks through Napro B2M valves for pressure reduction and a minimum of six feet of copper tubing to allow the gas to reach ambient temperature. To prevent the blowing out of manometer fluid during adjustment periods, three-way Teflon stopcocks are used to connect the manometers to the high pressure side of the capillaries. Tank regulators used for the various tank heads and pressures are those recommended by the Matheson Company.

The diffusion cell as assembled is shown in Figures 2 and 3. The glass parts of the cell were made in the Oklahoma State University Chemistry Department Glass Shop. The design follows that suggested by Rothfeld (46).

The cell is divided into two chambers by a copper ring in which the sample pellet is mounted. Inlet gases are directed toward each face of the sample pellet by the inner glass tubes, and outlet gases are removed through annular space around the inner tubes. To assure there is no static pressure difference across the pellet, an R G I Positive Closed End Manometer filled T.E.G. is connected to the two chambers separated by the pellet. Absolute pressure in the cell is measured using a 30-inch glass U-tube filled with mercury. The pressure on each side of the pellet is regulated by Napro Micro-Metering valves in the outlet stream lines.

The carbon pellets are wrapped around the circumference in a very thin film of Teflon tape and fitted into specially made brass rings. The tape assures no open spaces between the surface of the pellet and the inside surface of the annular brass rings. The brass ring is mounted in Tygon tubing, which is used to connect the two chambers

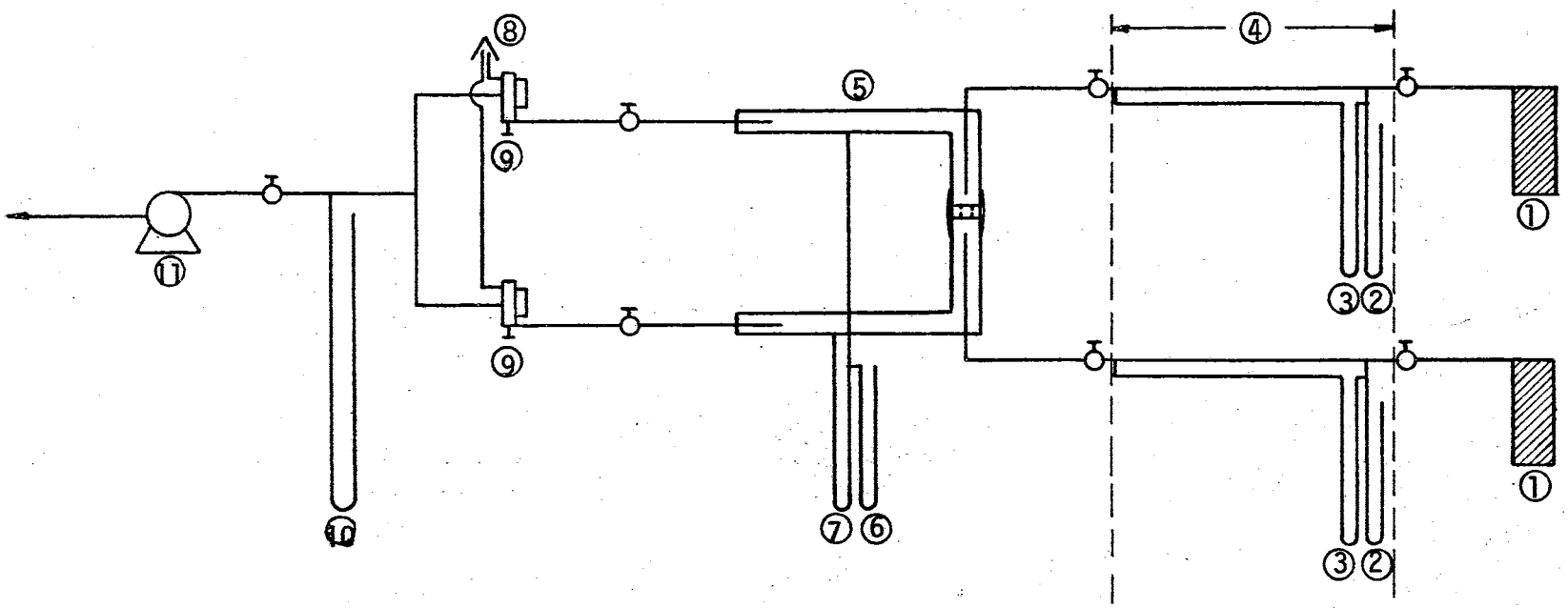

1. Gas Supply Tanks
2. Mercury Manometer
3. TEG Manometer
4. Capillary Flowmeters
5. Diffusion Cell
6. Mercury Manometer
7. TEG Manometer
8. Gas Chromatograph
9. Sampling Valve
10. Mercury Manometer
11. Vacuum Pump

Figure 2. Experimental System

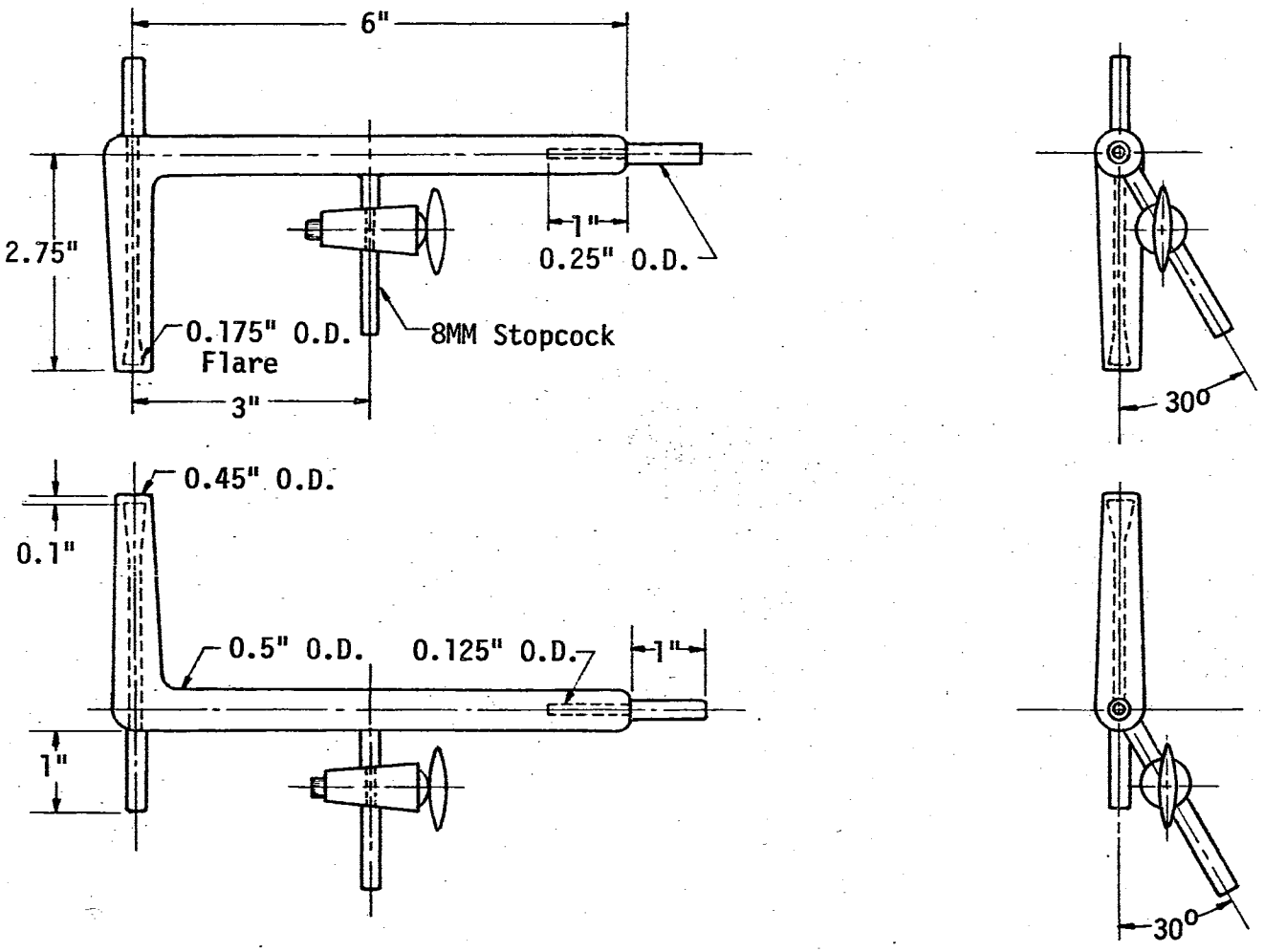

Figure 3. Diffusion Cell -- Details of Glass Parts

together and seal the cell. The cell is connected to the rest of the system with Swaglock union. The unions are connected on one side to the glass diffusion cell by means of Teflon ferrules and on the other side to Tygon tubing.

The use of short lengths of flexible tubing is necessary to prevent stress on the glass cell. The total volume of the system is small enough to allow it to be flushed in about 30 seconds (the gases enter at the rate of one to three cubic centimeters per second).

The gas analyzer module is a Micro-Tek GC 2500R gas chromatograph equipped with Micro-Tek's standard thermoconductivity cell and the recommended Honeywell recording potentiometer. The two chromatograph columns are packed with 20 grams each of Porapak Type Q, 50-80 mesh, in 1/4-inch copper tubing. A sample may be injected into either column for separation while the other is used as a reference. Each column is connected to a side of the diffusion cell.

Sampling of the outlet gases is done with two Micro-Tek linear gas sampling valves (catalog number 713107) connected directly to the exit lines of the diffusion cell. The valves allow a set volume of sample to be taken and injected into the chromatograph without any chance of contamination. Small volume sample loops were used to prevent flooding of the chromatograph columns. The size used was selected by a trial and error procedure. The pressure in the sampling valves and related cell outlet gas lines was regulated by a Napro Micro-Metering valve. The pressure was measured by a closed-end U-tube manometer during runs and by a Texas Instruments quartz tube precision pressure gauge during calibration.

A Duo Seal vacuum pump was used to maintain a low pressure at the exhaust end of the system.

All manometer levels are read with a precision cathetometer to $\pm$0.01 centimeter.

Procedure

The activated carbon pellets are prepared for runs by three operations, measuring, mounting, and regenerating. A cylindrical pellet having no noticeable cracks or bubbles is selected and its diameter is measured. An annular shaped brass disk is cut to the following dimensions, the outer diameter is 0.01 inch larger than the diameter of outer glass tubes of the diffusion cell; the inner diameter is 0.002 inch larger than measured diameter of the pellet; and the thickness is desired thickness of the pellet. The pellet is wrapped with a very thin film of Teflon tape and pushed into the disk. The excess tape is cut off and the pellet is filed level with the brass ring. The thickness of the pellet is then measured.

The mounted pellet is reactivated and stripped of adsorbed gases by a vacuum and high temperature treatment. The pellet is placed in a gas sample bomb which is connected to a vacuum pump. The vacuum pump is turned on and the bomb is placed in an oven at 150^{o} C for 24 hours. The oven is then turned off and the bomb is allowed to cool. The pellet is removed and slid into a length of Tygon tubing which is then used to connect and seal the diffusion cell chambers and hold the pellet in place. The system is put under vacuum for 24 hours to further degas the carbon. A vacuum is kept on the system whenever a run is not being made.

The gas chromatograph is turned on according to directions and the temperatures and carrier gas flow rates are adjusted, and allowed to reach a steady state. The chromatograph is calibrated as stated in Appendix B.

To make a run to measure diffusion flux rates, the procedure is as follows. The vacuum pump is turned on and all the control valves between the pump and the cell are opened. The gas tanks are opened and the pressures in the capillary flowmeters are regulated to approximately 10 p.s.i.a. The positive closed end manometer is closed. The valves between the flowmeters and the cell are opened to allow flow through the system. The Positive Closed End Manometer is opened and the pressures in the chambers of the pellet are set and equalized by adjusting the Micro-Metering valves in the outlet gas lines. The pressure in the chromatograph sampling valves is adjusted to approximately 2 p.s.i.a. by the Micro-Metering valve in the exhaust gas line.

After 10 minutes, a sample is injected into the chromatograph and a check is made on the compositions. (The lesser component should be between 1 and 3 percent.) If the concentrations of the diffusing gases are too large or too small, the flow rates of the experimental gases are readjusted and the above pressure adjustments are repeated. This is done until the concentration and pressures are as desired.

The system is allowed to run for 60 minutes to achieve steady state. A chromatograph sample is then taken every 15 minutes until the constant compositions occur. Then steady state is assumed to be reached and three pairs of samples are injected into the chromatograph. The levels of the manometers are read with the cathetometer and the ambient temperature is noted.

Using the readings taken as above, the outlet gas concentration, flow rates, pressure, and flux rates are calculated as shown in Appendix D.

CHAPTER IV

DATA AND RESULTS

Columbia Activated Carbon Type NXC 4/6 was used in this investigation. Physical properties of this type of carbon were analyzed by the manufacturer and are shown in Table XXVII and Figure 10. The pore size distribution below a diameter of 18 $\overset{o}{A}$ is not available, but the average pore size was assumed to be 9 $\overset{o}{A}$ in this range. The average pore sizes for the macro- and micropore regions were calculated from the pore distribution by a volume average. A numerical integration was used

$$\bar{r} = \sum_i r_i \; v_i \Big/ \sum_i v_i \qquad (41)$$

The point of separation between macro- and micropores was chosen at 150 $\overset{o}{A}$ after several points were tried. This is found to give the Wakao and Smith model the best fit to the helium-nitrogen data. Neither helium nor nitrogen is adsorbed enough to exhibit significant surface mass transfer.

The temperature of the runs was ambient temperature which was nearly constant at 25^{o} C in the air-conditioned laboratory. The cell pressure ranged from 58 to 718 m.m. mercury. The concentrations at the faces of the pellets were between 0% and 5%.

Tables I, II and III present the experimental data for the various runs. The concentrations are listed as attenuations and peak heights of the chromatograph peaks. The flow rates of the pure gases are calculated, as described in Appendix A, from the manometer readings.

Tables IV, V and VI show the quantities directly calculated from the experimental data. The mole fractions are calculated by the method shown in Appendix B. The fluxes were determined from a material balance around the cell as shown in Appendix D. The effective diffusivity is defined using an equation of the same form as Fick's Law and considering the pellet an open space in the brass ring in which the pellet is mounted. The concentrations at the pellet faces are assumed to be the outlet gas concentrations. Table VII shows values for methane-propane systems which were obtained by Denenholz (21) on the same apparatus. They are included here for convenient reference in subsequent discussions.

Tables VIII, IX, X and XI show values of the Wakao and Smith model calculation. The bulk diffusivities were calculated by the method of Fuller, Schettler and Giddings when values were not available in the literature. The Knudsen diffusivities were calculated from Equation (3) with K_o equal to 2/3. The fluxes and flux ratios were calculated using the long form of the Wakao and Smith model, Equation (16). The effective diffusivities were calculated in the same manner as those in the previous tables.

Tables XII, XIII, XIV and XV show surface fluxes calculated from the experimental data in two different ways. Method A assumes that the Wakao and Smith model predicts the gas phase flux accurately. The difference between the observed and predicted flux of propane is taken as the surface flux. Method B assumes that methane and helium do not exhibit surface flux. The gas phase flux of propane is calculated by multiplying the flux of methane or helium by the theoretical ratio of gas phase fluxes given in Equation (8). The difference between the

TABLE I

He - N_2 DATA

Pellet Area = 0.156 cm^2

Pellet Length = 0.312 cm

Run	Temp. (^oC)	Cell Pressure (mm Hg)	Chromatograph Analysis: Valve 1 He Att.	Valve 1 He P.H.	Valve 1 N_2 Att.	Valve 1 N_2 P.H.	Valve 2 He Att.	Valve 2 He P.H.	Valve 2 N_2 Att.	Valve 2 N_2 P.H.	Flow Rate Pure He X 10^5 $\left(\frac{g\ moles}{sec.}\right)$	Flow Rate Pure N_2 X 10^5 $\left(\frac{g\ moles}{sec.}\right)$
1	24.0	58.0	8	16.2	8	1.85	1	3.45	16	17.1	0.810	0.779
2	24.3	157.2	8	38.8	8	3.27	1	5.43	16	41.6	1.569	1.942
3	24.0	237.6	8	38.1	8	3.38	1	6.15	16	40.6	1.331	1.882
4	23.8	375.8	8	35.3	8	4.58	1	6.13	16	37.7	1.132	1.940
5	23.8	535.6	8	38.3	8	6.40	1	5.50	16	41.4	0.979	2.444
6	24.0	717.7	8	41.6	8	5.05	1	6.20	16	44.4	1.556	2.333

TABLE II

He - C_3H_8 DATA

Pellet Area = 0.156 cm^2

Pellet Length = 0.312 cm

Run	Temp. (^oC)	Cell Pressure (mm Hg)	Chromatograph Analysis: Valve 1 He Att.	Valve 1 He P.H.	Valve 1 C_3H_8 Att.	Valve 1 C_3H_8 P.H.	Valve 2 He Att.	Valve 2 He P.H.	Valve 2 C_3H_8 Att.	Valve 2 C_3H_8 P.H.	Flow Rate Pure He X 10^5 $\left(\frac{g\ moles}{sec.}\right)$	Flow Rate Pure C_3H_8 X 10^5 $\left(\frac{g\ moles}{sec.}\right)$
1	24.0	131.6	8	39.8	2	3.90	1	3.15	4	48.2	1.837	1.788
2	24.0	250.5	8	31.9	2	4.43	1	2.03	4	40.3	1.491	2.183

TABLE III

CH_4 - C_3H_8 DATA

Pellet Area = 0.156 cm^2

Pellet Length = 0.312 cm

Run	Temp. (^oC)	Cell Pressure (mm Hg)	Chromatograph Analysis: Valve 1 CH_4 Att.	Valve 1 CH_4 P.H.	Valve 1 C_3H_8 Att.	Valve 1 C_3H_8 P.H.	Valve 2 CH_4 Att.	Valve 2 CH_4 P.H.	Valve 2 C_3H_8 Att.	Valve 2 C_3H_8 P.H.	Flow Rate Pure CH_4 X 10^5 $\left(\frac{g\ moles}{sec.}\right)$	Flow Rate Pure C_3H_8 X 10^5 $\left(\frac{g\ moles}{sec.}\right)$
1	25.0	91.5	32	29.9	2	5.50	2	1.3	4	34.8	0.6283	1.4531
2	25.0	85.9	32	26.7	2	5.40	2	2.10	4	31.1	0.6610	1.009
3	25.0	84.0	32	22.9	2	3.85	2	3.50	4	25.9	0.6560	0.4791
4	25.0	288.6	32	29.4	2	7.20	2	2.60	4	34.3	0.6294	0.8671
5	25.0	512.5	32	38.0	2	3.90	2	6.26	4	41.9	1.5260	0.5010
6	25.0	685.0	32	38.1	2	4.30	2	2.26	4	42.5	1.4212	1.4102

TABLE IV

$He - N_2$ SYSTEM

Calculated Quantities

Run	$Y_{He,o}$	$Y_{He,L}$	Helium Flux $N_{He} \times 10^5$ $\left(\frac{g\ moles}{cm^2\ sec.}\right)$	Nitrogen Flux $N_{N_2} \times 10^5$ $\left(\frac{g\ moles}{cm^2\ sec.}\right)$	N_{He}/N_{N_2}	D_{EFF} $\left(\frac{cm^2}{sec.}\right)$	$P\ D_{EFF}$ $\left(\frac{cm^2 \cdot mm\ Hg}{sec.}\right)$
1	0.9789	0.0455	0.2347	0.1072	2.189	0.17646	10.23
2	0.9844	0.0300	0.3822	0.1532	2.495	0.09832	15.45
3	0.9835	0.0346	0.4305	0.1361	3.164	0.06674	15.85
4	0.9761	0.0370	0.4743	0.1665	2.850	0.04917	18.48
5	0.9695	0.0304	0.4890	0.1830	2.672	0.03676	19.69
6	0.9776	0.0320	0.4901	0.2182	2.246	0.02919	20.95

TABLE V

He - C_3H_8 SYSTEM

Calculated Quantities

Run	$Y_{He,o}$	$Y_{He,L}$	Helium Flux $N_{He} \times 10^5$ $\left(\frac{g\ moles}{cm^2\ sec.}\right)$	Propane Flux $H_{C_3H_8} \times 10^5$ $\left(\frac{g\ moles}{cm^2\ sec.}\right)$	$N_{He}/N_{C_3H_8}$	D_{EFF} $\left(\frac{cm^2}{sec.}\right)$	$P\ D_{EFF}$ $\left(\frac{cm^2 \cdot mm\ Hg}{sec.}\right)$
1	0.9692	0.0182	0.2087	0.3691	0.5656	0.13220	17.40
2	0.9568	0.0142	0.1971	0.4242	0.4646	0.07344	18.39

TABLE VI

CH_4 - C_3H_8 SYSTEM

Calculated Quantities

Run	$Y_{CH_4,o}$	$Y_{CH_4,L}$	Methane Flux $N_{CH_4} \times 10^6$ $\left(\frac{\text{g moles}}{\text{cm}^2 \text{ sec.}}\right)$	Propane Flux $N_{C_3H_8} \times 10^6$ $\left(\frac{\text{g moles}}{\text{cm}^2 \text{ sec.}}\right)$	$N_{CH_4}/N_{C_3H_8}$	D_{EFF} $\left(\frac{\text{cm}^2}{\text{sec.}}\right)$	$P\ D_{EFF}$ $\left(\frac{\text{cm}^2 \cdot \text{mm Hg}}{\text{sec.}}\right)$
1	0.9694	0.0051	0.4754	1.262	0.3767	0.05353	4.898
2	0.9663	0.0092	0.5912	1.462	0.4044	0.06869	5.900
3	0.9718	0.0182	0.5524	1.207	0.4576	0.06184	5.192
4	0.9595	0.0103	0.5659	1.685	0.3359	0.02195	6.336
5	0.9826	0.0198	0.6192	1.723	0.3595	0.01303	6.676
6	0.9810	0.0072	0.6540	1.760	0.3716	0.00989	6.774

TABLE VII

CH_4 - C_3H_8 SYSTEM

Denenholz' Calculated Quantities

Pellet Area = 0.146 cm^2

Run	Temp. (^oC)	Pressure (mm Hg)	$Y_{CH_4,o}$	$Y_{C_3H_8,L}$	Pellet Length (cm)	Methane Flux $N_{CH_4} \times 10^6$ $\left(\frac{g\ moles}{cm^2\ sec.}\right)$	Propane Flux $N_{C_3H_8} \times 10^5$ $\left(\frac{g\ moles}{cm^2\ sec.}\right)$	$N_{CH_4}/N_{C_3H_8}$	D_{EFF} $\left(\frac{cm^2}{sec.}\right)$	P D_{EFF} $\left(\frac{cm^2 \cdot mm\ Hg}{sec.}\right)$
1	24.5	734.9	0.9785	0.0038	0.3556	0.295	0.244	0.121	0.009327	6.855
2	25.0	104.1	0.9662	0.0090	0.3556	0.780	0.113	0.690	0.06233	6.490
3	25.0	236.4	0.9715	0.0085	0.3556	0.668	0.151	0.442	0.02983	7.051
4	25.0	351.9	0.9883	0.0088	0.3556	0.650	0.157	0.414	0.02003	7.048
5	25.0	741.0	0.9775	0.0020	0.3556	0.202	0.320	0.063	0.009868	7.312
6	26.0	107.9	0.9802	0.0030	0.3759	0.299	0.196	0.153	0.05092	5.495
7	25.3	761.5	0.9787	0.0020	0.3759	0.311	0.260	0.120	0.01006	7.661
8	24.5	737.2	0.9797	0.0137	0.3759	0.287	0.248	0.116	0.01018	7.503
9	25.3	752.4	0.9866	0.0097	0.3759	0.386	0.268	0.144	0.01140	8.580

TABLE VII (Continued)

Run	Temp. (^{o}C)	Pressure (mm Hg)	$Y_{CH_4,o}$	$Y_{C_3H_8,L}$	Pellet Length (cm)	Methane Flux $N_{CH_4} \times 10^6$ $\left(\frac{g\ moles}{cm^2\ sec.}\right)$	Propane Flux $N_{C_3H_8} \times 10^5$ $\left(\frac{g\ moles}{cm^2\ sec.}\right)$	$N_{CH_4}/N_{C_3H_8}$	D_{EFF} $\left(\frac{cm^2}{sec.}\right)$	$P\ D_{EFF}$ $\left(\frac{cm^2 \cdot mm\ Hg}{sec.}\right)$
10	25.0	107.9	0.9800	0.0035	0.3759	0.346	0.169	0.205	0.04941	5.332
11	25.0	468.2	0.9840	0.0048	0.3759	0.279	0.240	0.116	0.01505	7.045
12	24.8	105.6	0.9752	0.0136	0.2515	0.494	0.145	0.341	0.04091	4.322
13	24.8	189.2	0.9855	0.0329	0.2515	0.490	0.152	0.322	0.02412	4.564
14	25.0	183.2	0.9857	0.0034	0.2515	0.594	0.181	0.328	0.02831	5.184
15	25.0	452.2	0.9799	0.0080	0.2515	0.665	0.134	0.496	0.01024	4.632
16	25.5	104.9	0.9737	0.0060	0.2515	0.609	0.133	0.458	0.04241	4.448

TABLE VIII

He - N_2 SYSTEM

Wakao-Smith Gas Diffusion Model

Run	$D^*_{He-N_2}$	D_{Ka}		$D_{Ki} \times 10^3$		$N_{He} \times 10^5$	$N_{N_2} \times 10^5$	N_{He}/N_{N_2}	D_{EFF}	$P\ D_{EFF}$
		He	N_2	He	N_2					
	$\left(\frac{cm^2}{sec.}\right)$	$\left(\frac{cm^2}{sec.}\right)$	$\left(\frac{cm^2}{sec.}\right)$	$\left(\frac{cm^2}{sec.}\right)$	$\left(\frac{cm^2}{sec.}\right)$	$\left(\frac{g\ moles}{cm^2\ sec.}\right)$	$\left(\frac{g\ moles}{cm^2\ sec.}\right)$		$\left(\frac{cm^2}{sec.}\right)$	$\left(\frac{cm^2 \cdot mm\ Hg}{sec.}\right)$
1	8.978	7.4700	2.823	4.840	1.829	0.2155	0.0815	2.646	0.14702	8.512
2	3.315	7.474	2.825	4.842	1.830	0.3757	0.1420	2.646	0.09265	14.55
3	2.189	7.470	2.823	4.840	1.829	0.4362	0.1649	2.646	0.07141	16.96
4	1.382	7.468	2.822	4.838	1.829	0.4909	0.1856	2.646	0.05150	19.35
5	0.9696	7.467	2.822	4.838	1.829	0.5280	0.1996	2.646	0.03914	20.96
6	0.7243	7.470	2.823	4.840	1.829	0.5634	0.2129	2.646	0.03078	22.09

*Reference 43.

TABLE IX

$He - C_3H_8$ SYSTEM

Wakao-Smith Gas Diffusion Model

Run	$D^*_{He-C_3H_8}$	D_{Ka}		$D_{Ki} \times 10^3$		$N_{He} \times 10^5$	$N_{C_3H_8} \times 10^6$	$N_{He}/N_{C_3H_8}$	D_{EFF}	$P\ D_{EFF}$
		He	C_3H_8	He	C_3H_8					
	$\left(\frac{cm^2}{sec.}\right)$	$\left(\frac{cm^2}{sec.}\right)$	$\left(\frac{cm^2}{sec.}\right)$	$\left(\frac{cm^2}{sec.}\right)$	$\left(\frac{cm^2}{sec.}\right)$	$\left(\frac{g\ moles}{cm^2\ sec.}\right)$	$\left(\frac{g\ moles}{cm^2\ sec.}\right)$		$\left(\frac{cm^2}{sec.}\right)$	$\left(\frac{cm^2 \cdot mm\ Hg}{sec.}\right)$
1	2.160	7.472	2.250	4.842	1.458	0.2494	0.7512	3.321	0.06849	9.014
2	1.135	7.472	2.250	4.842	1.458	0.2943	0.8862	3.321	0.04338	10.863

*Estimated by the method of Fuller, Schettler and Giddings (43).

TABLE X

CH_4 - C_3H_8 SYSTEM

Wakao-Smith Gas Diffusion Model

Run	$D^*_{CH_4\text{-}C_3H_8}$ $\left(\frac{cm^2}{sec.}\right)$	D_{Ka} CH_4 $\left(\frac{cm^2}{sec.}\right)$	D_{Ka} C_3H_8 $\left(\frac{cm^2}{sec.}\right)$	$D_{Ki} \times 10^3$ CH_4 $\left(\frac{cm^2}{sec.}\right)$	$D_{Ki} \times 10^3$ C_3H_8 $\left(\frac{cm^2}{sec.}\right)$	$N_{CH_4} \times 10^6$ $\left(\frac{g\ moles}{cm^2\ sec.}\right)$	$N_{C_3H_8} \times 10^6$ $\left(\frac{g\ moles}{cm^2\ sec.}\right)$	$N_{CH_4}/N_{C_3H_8}$	D_{EFF} $\left(\frac{cm^2}{sec.}\right)$	$P\ D_{EFF}$ $\left(\frac{cm^2 \cdot mm\ Hg}{sec.}\right)$
1	1.079	3.737	2.254	2.421	1.460	0.7335	0.4424	1.6578	0.03816	3.492
2	1.150	3.737	2.254	2.421	1.460	0.7149	0.4313	1.6578	0.03992	3.429
3	1.177	3.737	2.254	2.421	1.460	0.7093	0.4278	1.6578	0.04053	3.403
4	0.3422	3.737	2.254	2.421	1.460	0.9076	0.5475	1.6578	0.01524	4.398
5	0.1927	3.737	2.254	2.421	1.460	1.001	0.6039	1.6578	0.00925	4.740
6	0.1442	3.737	2.254	2.421	1.460	1.048	0.6323	1.6578	0.00719	4.922

*Estimated by the method of Fuller, Schettler and Giddings (43).

TABLE XI

CH_4 - C_3H_8 SYSTEM

Denenholz Data

Wakao-Smith Gas Diffusion Model

Run	$D^*_{CH_4-C_3H_8}$ $\left(\frac{cm^2}{sec.}\right)$	D_{Ka} CH_4 $\left(\frac{cm^2}{sec.}\right)$	D_{Ka} C_3H_8 $\left(\frac{cm^2}{sec.}\right)$	$D_{Ki} \times 10^3$ CH_4 $\left(\frac{cm^2}{sec.}\right)$	$D_{Ki} \times 10^3$ C_3H_8 $\left(\frac{cm^2}{sec.}\right)$	$N_{CH_4} \times 10^6$ $\left(\frac{g\ moles}{cm^2\ sec.}\right)$	$N_{C_3H_8} \times 10^6$ $\left(\frac{g\ moles}{cm^2\ sec.}\right)$	$N_{CH_4}/N_{C_3H_8}$	D_{EFF} $\left(\frac{cm^2}{sec.}\right)$	$P\ D_{EFF}$ $\left(\frac{cm^2 \cdot mm\ Hg}{sec.}\right)$
1	0.1340	3.733	2.252	2.419	1.459	0.9271	0.5592	1.6578	0.00674	4.956
2	0.9486	3.737	2.254	2.421	1.460	0.6615	0.3990	1.6578	0.03473	3.616
3	0.4179	3.737	2.254	2.421	1.460	0.7861	0.4742	1.6578	0.01805	4.266
4	0.2807	3.737	2.254	2.421	1.460	0.8505	0.5130	1.6578	0.01283	4.514
5	0.1333	3.737	2.254	2.421	1.460	0.9292	0.5605	1.6578	0.00671	4.976
6	0.9206	3.743	2.258	2.425	1.463	0.6469	0.3902	1.6578	0.03395	3.664
7	0.1299	3.738	2.255	2.422	1.461	0.8842	0.5333	1.6578	0.00657	5.002
8	0.1336	3.733	2.252	2.419	1.459	0.8714	0.5257	1.6578	0.00672	4.957

*Estimated by the method of Fuller, Schettler and Giddings (43).

TABLE XI (Continued)

Run	$D^{*}_{CH_4-C_3H_8}$ $\left(\frac{cm^2}{sec.}\right)$	D_{Ka} CH_4 $\left(\frac{cm^2}{sec.}\right)$	D_{Ka} C_3H_8 $\left(\frac{cm^2}{sec.}\right)$	$D_{Ki} \times 10^3$ CH_4 $\left(\frac{cm^2}{sec.}\right)$	$D_{Ki} \times 10^3$ C_3H_8 $\left(\frac{cm^2}{sec.}\right)$	$N_{CH_4} \times 10^6$ $\left(\frac{g\ moles}{cm^2\ sec.}\right)$	$N_{C_3H_8} \times 10^6$ $\left(\frac{g\ moles}{cm^2\ sec.}\right)$	$N_{CH_4}/N_{C_3H_8}$	D_{EFF} $\left(\frac{cm^2}{sec.}\right)$	$P\ D_{EFF}$ $\left(\frac{cm^2 \cdot mm\ Hg}{sec.}\right)$
9	0.1315	3.738	2.255	2.422	1.461	0.8860	0.5344	1.6578	0.00663	4.991
10	0.9152	3.737	2.254	2.421	1.460	0.6456	0.3894	1.6578	0.00379	3.646
11	0.2110	3.737	2.254	2.421	1.460	0.8333	0.5027	1.6578	0.01001	4.687
12	0.9339	3.735	2.253	2.420	1.460	0.9454	0.5703	1.6578	0.03429	3.623
13	0.5213	3.735	2.253	2.420	1.460	1.0674	0.6439	1.6578	0.02166	4.099
14	0.5392	3.737	2.254	2.421	1.460	1.0888	0.6568	1.6578	0.02230	4.084
15	0.2184	3.737	2.254	2.421	1.460	1.2302	0.7420	1.6578	0.01032	4.666
16	0.9445	3.740	2.256	2.423	1.462	0.9490	0.5725	1.6578	0.03461	3.630

TABLE XII

He - C_3H_8 SYSTEM

Surface Diffusion

Run	$N_{C_3H_8} \times 10^5$			$N_{S,C_3H_8} \times 10^5$		$D_{S,C_3H_8} \times 10^3$			
						METHOD A		METHOD B	
	EXP.	EQN. 16	EQN. 8	METHOD A	METHOD B	EQN. 37	EQN. 40	EQN. 37	EQN. 40
1	0.369	0.075	0.063	0.294	0.306	0.535	0.834	0.557	0.688
2	0.424	0.089	0.059	0.336	0.365	0.678	0.749	0.737	0.814

TABLE XIII

CH_4 - C_3H_8 SYSTEM

Surface Diffusion

	$N_{C_3H_8}$ X 10^6			N_{S,C_3H_8} X 10^6		D_{S,C_3H_8} X 10^3			
						METHOD A		METHOD B	
Run	EXP.	EQN. 16	EQN. 8	METHOD A	METHOD B	EQN. 37	EQN. 40	EQN. 37	EQN. 40
1	1.262	0.442	0.287	0.820	0.975	0.187	0.282	0.222	0.335
2	1.462	0.431	0.356	1.030	1.106	0.252	0.375	0.271	0.403
3	1.207	0.428	0.333	0.779	0.874	0.193	0.283	0.217	0.318
4	1.685	0.548	0.341	1.137	1.344	0.140	0.242	0.165	0.286
5	1.723	0.604	0.373	1.119	1.312	0.087	0.195	0.102	0.229
6	1.760	0.632	0.394	1.128	1.366	0.102	0.170	0.134	0.206

TABLE XIV

CH_4 - C_3H_8 SYSTEM

Denenholz Data

Surface Diffusion

Run	$N_{C_3H_8}$ X 10^6			N_{S,C_3H_8} X 10^6		$D_{S,\ C_3H_8}$ X 10^3			
						METHOD A		METHOD B	
	EXP.	EQN. 16	EQN. 8	METHOD A	METHOD B	EQN. 37	EQN. 40	EQN. 37	EQN. 40
1	2.44	0.56	0.18	1.88	2.26	0.191	0.362	0.230	0.436
2	1.13	0.40	0.47	0.83	0.66	0.193	0.303	0.153	0.241
3	1.51	0.47	0.40	1.04	1.11	0.144	0.258	0.153	0.275
4	1.57	0.51	0.39	1.06	1.18	0.133	0.262	0.148	0.291
5	3.20	0.56	0.12	2.64	3.08	0.268	0.513	0.312	0.598
6	1.96	0.39	0.18	1.57	1.78	0.377	0.581	0.427	0.659
7	2.60	0.53	0.19	2.07	2.41	0.221	0.422	0.258	0.492
8	2.48	0.53	0.17	1.95	2.31	0.208	0.396	0.246	0.469
9	2.68	0.53	0.17	2.15	2.51	0.228	0.418	0.266	0.487
10	1.69	0.39	0.21	1.30	1.48	0.306	0.479	0.349	0.546
11	2.40	0.50	0.17	1.90	2.23	0.228	0.401	0.268	0.471

TABLE XIV (Continued)

Run	$N_{C_3H_8} \times 10^6$			$N_{S,C_3H_8} \times 10^6$		$D_{S,C_3H_8} \times 10^3$			
						METHOD A		METHOD B	
	EXP.	EQN. 16	EQN. 8	METHOD A	METHOD B	EQN. 37	EQN. 40	EQN. 37	EQN. 40
12	1.45	0.57	0.30	0.88	1.15	0.145	0.224	0.190	0.293
13	1.52	0.64	0.30	0.88	1.22	0.104	0.166	0.144	0.231
14	1.81	0.66	0.36	1.15	1.45	0.134	0.216	0.169	0.273
15	1.34	0.74	0.40	0.60	0.94	0.049	0.088	0.077	0.138
16	1.33	0.57	0.37	0.76	0.96	0.124	0.194	0.157	0.246

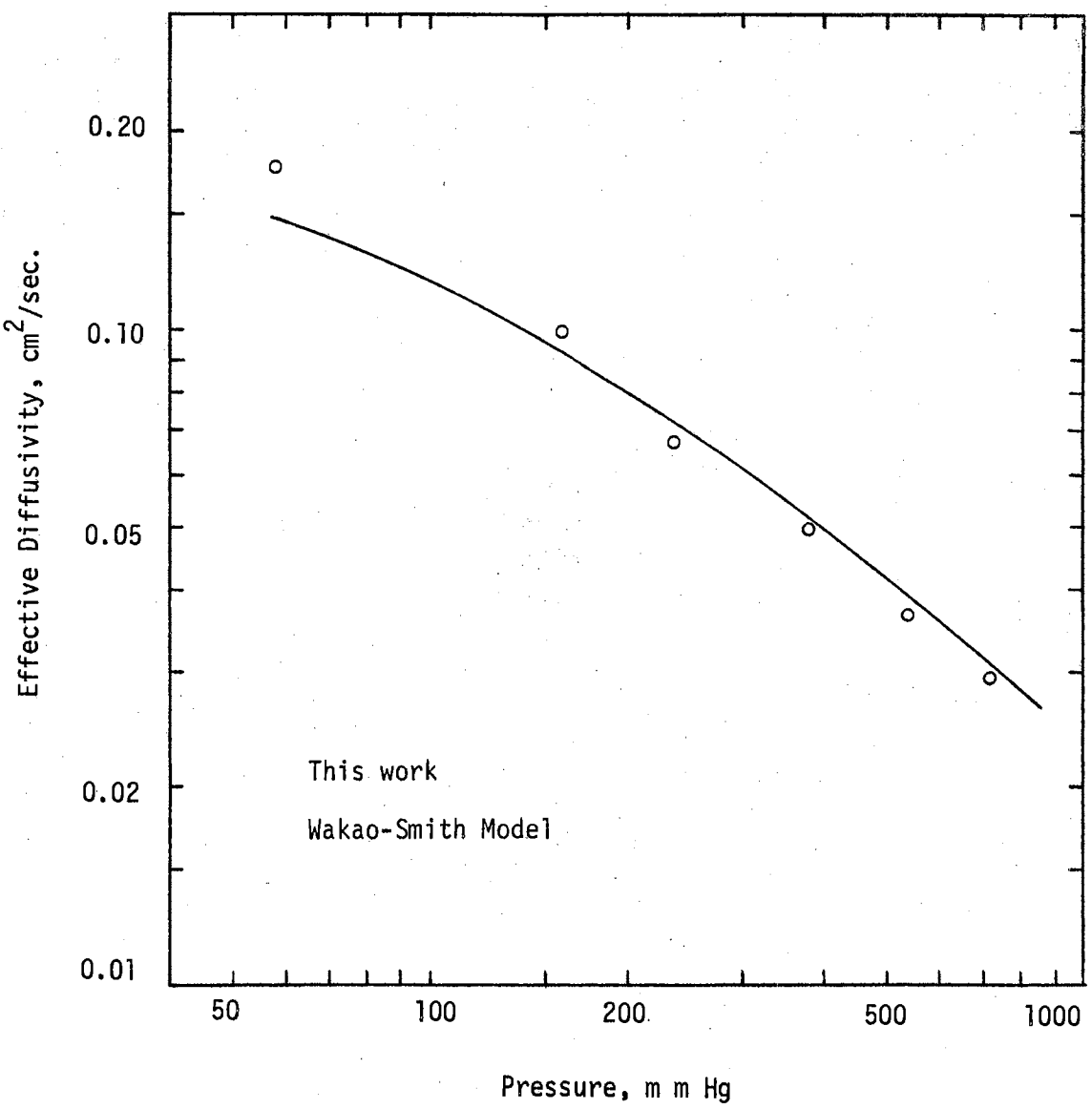

Figure 4. Helium-Nitrogen -- Effective Diffusivity Versus Pressure

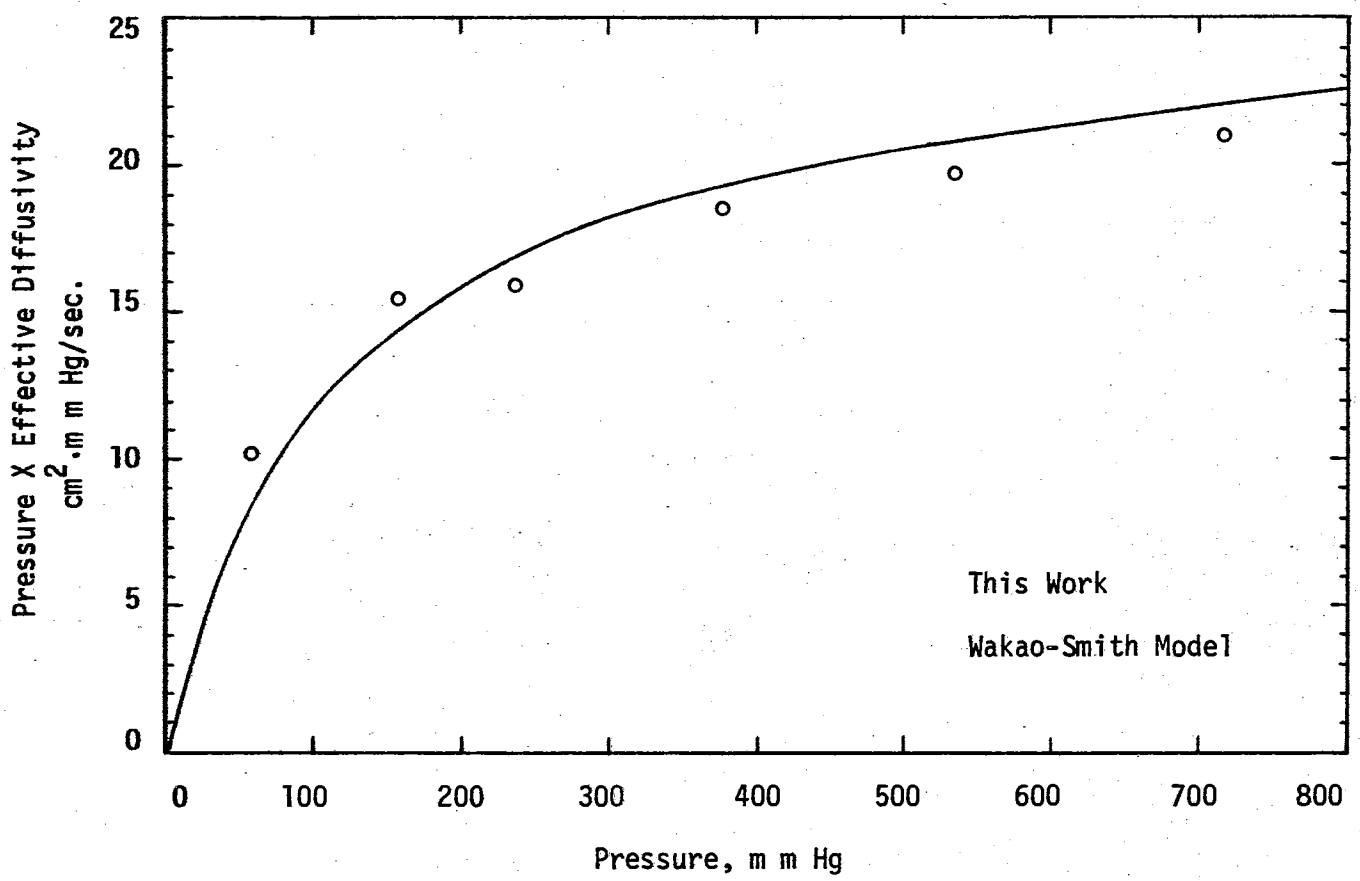

Figure 5. Helium-Nitrogen -- Pressure X Effective Diffusivity Versus Pressure

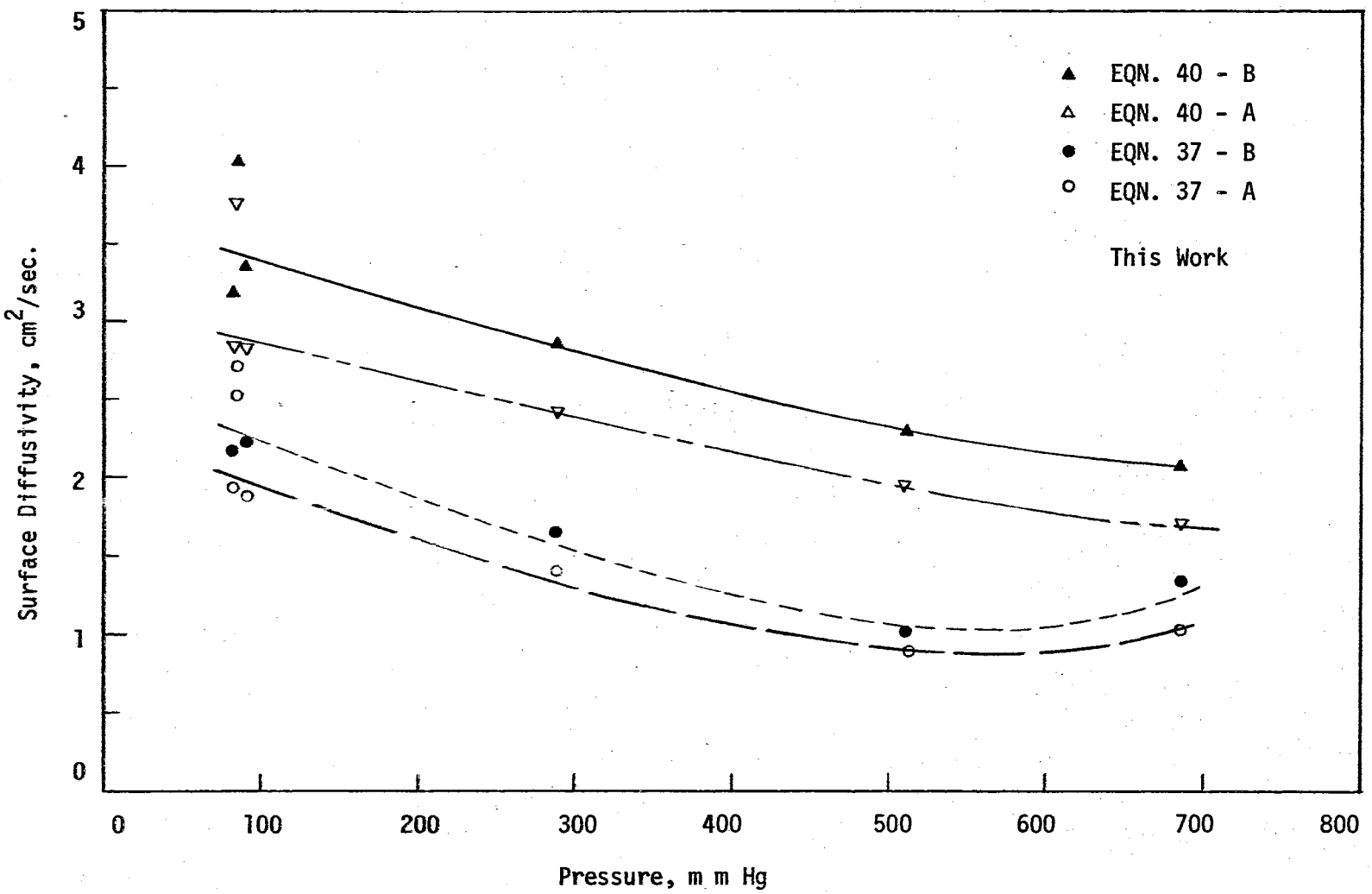

Figure 6. Propane Surface Diffusivity -- Comparison of Calculation Methods

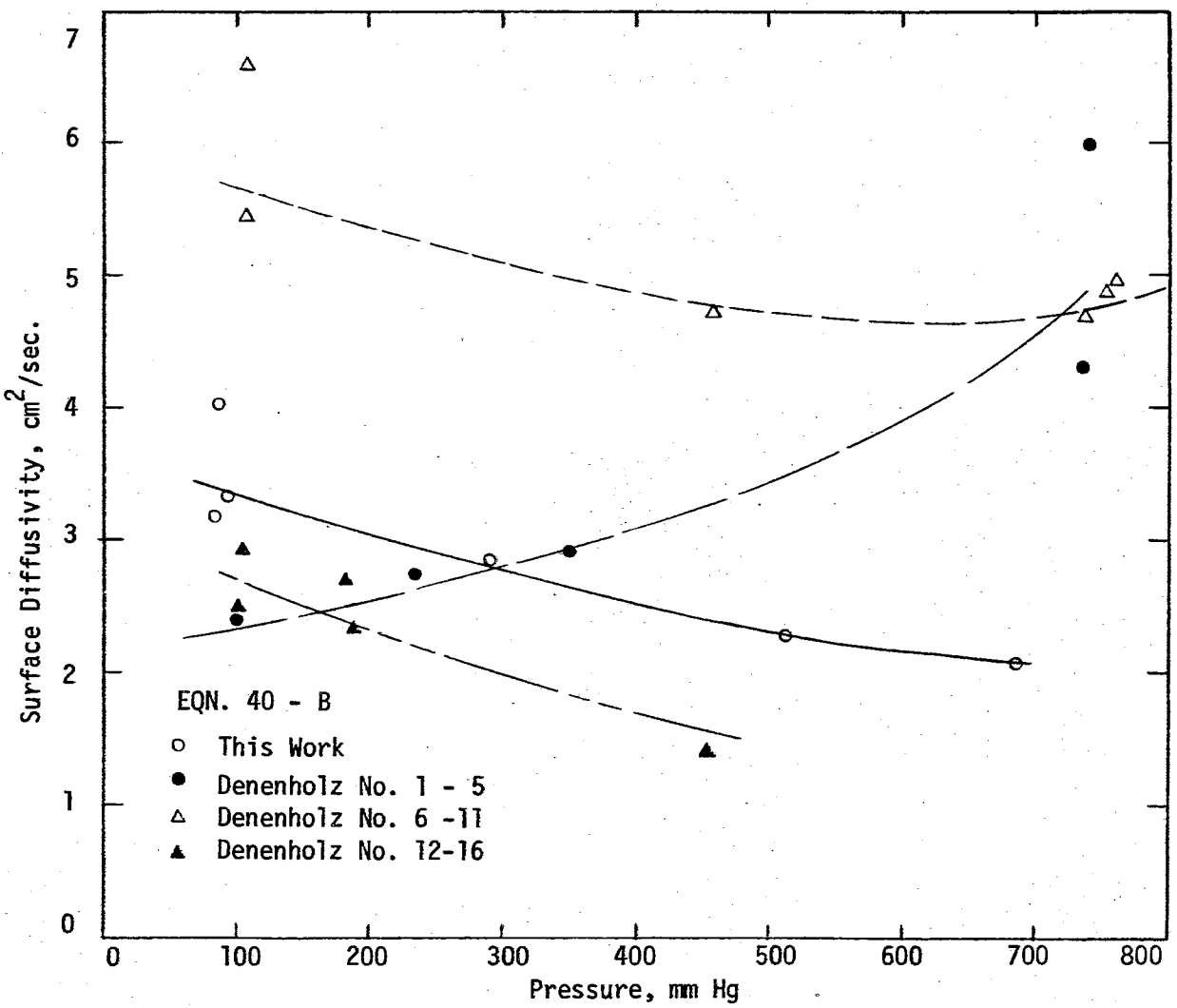

Figure 7. Propane Surface Diffusivity -- Comparison of Values in Different Pellets

observed and calculated flux of propane is taken as the surface flux. The surface diffusivities are calculated using Equations (37) and (40) for both methods of calculating surface flux. The value of $\overline{K}_S$ used in Equation (37) is found by

$$\overline{K}_S = \overline{C}' / C \tag{42}$$

where $\overline{C}'$ and C are the values at the average partial pressure across the pellet.

The effective diffusivities experimentally observed and those predicted by the Wakao and Smith model are shown in graphical form in Figures 4 and 5. The surface diffusivities are shown in Figures 6 and 7.

Discussion

The accuracy of the experimental diffusion fluxes depends on the flow rates of the pure gases and the concentrations of the inlet and outlet streams. The capillary flow meters used to measure the flow rates are accurate to $\pm 0.005 \times 10^{-3}$ g-moles/minute. This figure was arrived at through examination of the calibration data. Both inlet gases are assumed to contain no impurities since when passed through the gas chromatograph no peaks other than those of the pure gases were noted. The estimated error in composition of the exit streams is ± 0.001 mole fraction. This error is caused by small variations in the sample loop temperature and by the limitation of measuring the peak heights. An error analysis on the equations for the experimental fluxes show that the probable error in the flux rates is approximately ten percent. The accuracy of the surface fluxes is difficult to

TABLE XV

SURFACE DIFFUSIVITIES

Selected Literature Values

System	Temperature Range (°C)	Pressure Range (mm Hg)	$D_S \times 10^4$ (cm^2/sec.)	Reference
SO_2-Carbon	- 34 to 0	100 to 400	1.7 to 12.1	1
CO_2-Carbon	-83	50 to 500	0.9 to 2.6	1
N_2-Carbon	-196 to -183	50 to 500	1.9 to 3.7	1
A-Carbon	-196 to -183	20 to 200	0.5 to 0.9	1
CH_4-Silica Alumina Catalyst	0 to 180	760	2.6 to 69.1	10
C_2H_6-Silica Alumina Catalyst	103 to 180	760	2.6 to 22.3	10
C_3H_8-Silica Alumina Catalyst	103 to 180	760	2.5 to 8.6	10

estimate. If the Wakao-Smith model is assumed to be accurate, the subtraction to the observed fluxes and the predicted gas phase diffusion fluxes will lead to an average error of approximately 30 percent.

Further error is introduced when the accuracy of the predicted gas phase fluxes are questioned. The estimation of D_{A-B} for helium-propane and methane-propane has a probable accuracy of seven percent. The adsorbed layer on the walls of the pores may change the average pore size available to gas phase diffusion.

The surface diffusivity tends to decrease with pressure. This is attributed to molecules interfering with one another, since most adjacent sites are filled as the monolayer is approached, requiring a molecule to advance by entering the second layer -- a more energetic process. As the second layer becomes increasingly occupied, the flow rate again increases.

The fluxes of helium and methane predicted by the Wakao and Smith model are larger than those observed experimentally. This may be due to the limits of accuracy of model or the blockage of pores by the adsorbed gases. On this basis, it might be said that Method B gives more reliable surface fluxes than Method A.

Some surface diffusivities reported in the literature for adsorbed gases are listed in Table XV and are of the same order of magnitude as the values determined in this work. There is much published data on surface diffusion. An extensive list of articles may be found in the bibliography.

CHAPTER V

SUMMARY

Conclusions

Diffusional fluxes have been measured for several gas mixtures through an activated carbon pellet. These fluxes have been correlated by gaseous diffusion and surface diffusion models. Experiments with the non-adsorbing nitrogen helium system show that the Wakao-Smith bidisperse pore model predicts the gas phase fluxes through activated carbon reasonably well when surface mass transfer is not present. However, the model does not appear to predict gas phase flux of helium or methane very well when surface flux of propane is present. Several methods of evaluation of surface flux and surface diffusivity from the experimental data were tried. The preferred method uses the theoretical gas phase flux ratio to predict gas phase flux of the adsorbed gas, propane, and a surface flux-diffusivity correlation which uses the Langmuir adsorption isotherm.

Suggestions for Further Work

Surface diffusivities need to be measured over a wider pressure range than is done in this work to obtain a more complete relationship between pressure and diffusivity. The gas chromatographic method used to measure gas compositions was found to be limited in accuracy in the

lower pressure range and often trouble prone. A simpler and more versatile means of composition analysis is highly desirable.

A SELECTED BIBLIOGRAPHY

(1) Ash, R., Barrer, Pope. "Flow of Adsorbed Gases and Vapour in a Microporous Media. I. Single Sorbates." Proc. Roy. Soc. Vol. 271A. (1963) Page 1.

(2) Ash, R., Barrer, Pope. "Flow of Adsorbed Gases and Vapours in a Microporous Media. II. Binary Mixtures." Proc. Roy. Soc. Vol. 271A. (1963) Page 19.

(3) Babbitt, J. D. "On the Differential Equations of Diffusion." Can. J. Res. Vol. 28A. (1950) Page 449.

(4) Babbitt, J. D. "A Unified Picture of Diffusion." Can. J. Phy. Vol. 29. (1950) Page 427.

(5) Babbitt, J. D. "On the Diffusion of Adsorbed Gases Through Solids." Can. J. Phy. Vol. 29. (1950) Page 437.

(6) Barrer, R. M., Barrier, J. A. "Sorption and Surface Diffusion in Porous Glass." Proc. Roy. Soc. Vol. 213. (1952) Page 250.

(7) Barrer, R. M., Robins, A. B. Trans. Faraday Soc., Vol. 49. (1953) Page 429.

(8) Barrer, R. M., Robins, A. B. Trans. Faraday Soc., Vol. 49. (1953) Page 807.

(9) Barrer, R. M., Strachan, E. "Sorption and Surface Diffusion in Microporous Carbon Cylinders." Proc. Roy. Soc. Vol. 231A. (1955) Page 52.

(10) Barrer, R. M., Gabor, T. "Sorption and Diffusion of Simple Paraffins in Silica-Alumina Cracking Catalyst." Proc. Roy. Soc. Vol. 256A. (1960) Page 267.

(11) Bird, R. B., Stewart, W. E., Lightfoot, E. N. Transport Phenomena. New York: John Wiley and Sons, Inc. 1960.

(12) Brunauer, S., Deming, Deming, Teller. J. Am. Chem. Soc. Vol. 62. (1940) Page 1723.

(13) Brunauer, S. The Adsorption of Gases and Vapors. I. Physical Adsorption. Princeton: Princeton University Press, 1945.

(14) Carman, P. C., Malherbe, Poler. "Diffusion and Flow of Gases and Vapours Through Micropores. II. Surface Flow." Proc. Roy. Soc. Vol. 203A. (1950) Page 165.

(15) Carman, P. C., Raal, F. A. "Physical Adsorption of Gases on Porous Solids. I. Comparisons of Loose Powders and Porous Plugs." Proc. Roy. Soc. Vol. 209A. (1951) Page 38.

(16) Carman, P. C. "Diffusion and Flow of Gases and Vapours Through Micropores. I. Slip Flow and Molecular Streaming." Proc. Roy. Soc. Vol. 211A. (1952) Page 526.

(17) Continental Oil Company. Personal Communications.

(18) Darcey, J. R. "Surface Diffusion of Adsorbed Molecules." Ind. Eng. Chem. Vol. 57. (1965) Page 26.

(19) Dubinin, M. M. "The Porous Structure and Adsorption Properties of Active Carbons." Ind. Carbon and Graphite Soc. Chem. Ind. (1957) Pages 24-26.

(20) Emmett, P. H. Chem. Rev. 43:69. 1948.

(21) Denenholz, H. S. "Gaseous Binary Counterdiffusion in Activated Carbon." M.S. Thesis. Oklahoma State University (1967).

(22) Evans, R. B., Watson, G. M., Mason, E. A. "Gaseous Diffusion in Porous Media at Uniform Pressure." IMP-AEC 15. Inst. for Molecular Physics, University of Maryland (1961).

(23) Field, G. J., Watts, H., Weller, K. R. Revs. Pure and Appl. Chem. Vol. 13. (1963) Page 2.

(24) Flood, E. A., Tomlinson, R. H., Leger, A. E. "The Flow of Fluids Through Activated Carbon." Can. J. Chem. Vol. 30. (1952) Page 348.

(25) Flood, E. A., Tomlinson, R. H., Leger, A. E. "The Flow of Fluids Through Activated Carbon Rods. II. The Pore Structure of Activate RABS* Carbon." Can. J. Chem. Vol. 30. (1952) Page 372.

(26) Flood, E. A., Tomlinson, R. H., Leger, A. E. "The Flow of Fluids Through Activated Carbon. III. The Flow of Adsorbed Fluids." Can. J. Chem. Vol. 30. (1952) Page 389.

(27) Fowler, R. H., Guggenheim, E. M. Statistical Thermodynamics. London: The University Press (Cambridge), 1939.

(28) Gilliland, F. R., Baddour, Russell. "Rates of Flow Through Microporous Solids." A.I.Ch.E. J. Vol. 4. (1958) Page 90.

(29) Gilliland, E. R., Baddour, Engel. "Flow of Gases Through Porous Solids Under the Influence of Temperature Gradients." A.I.Ch.E. J. Vol. 8. (1962) Page 530.

(30) Gilliland, E. R., Baddour, Whang, Slader. "The Counterdiffusion of Adsorbed Hydrocarbons in Porous Glass." (1967).

(31) Heilman, W., Tammela, V., Meyer, J. A., Stannett, V., Szwarc, M. "Permeability of Polymer Films to Hydrogen Sulfide Gas." Ind. Eng. Chem. Vol. 48. (1956) Page 821.

(32) Henry, J. P., Cunningham, R. S., Geankoplis, C. J. "Diffusion of Gases in Porous Solids Over a Thousand-Fold Pressure Range." Chem. Eng. Sci. Vol. 22. (1967) Page 11.

(33) Hoogschagen, J. "Diffusion in Porous Catalysts and Adsorbents." Ind. Eng. Chem. Vol. 47. (1955) Page 906.

(34) Hwang, S. T., Kammermeyer, K. "Surface Diffusion in Microporous Media." Can. J. Chem. Eng. Vol. 44 (1966) Page 82.

(35) Hwang, S. T., Kammermeyer, K. "Surface Diffusion of Deuterium and Light Hydrocarbons in Microporous Vycor Glass." Separation Science. Vol. 1. (1966) Page 629.

(36) Hwang, S. T., Kammermeyer, K. "Evidence of Surface Diffusio of Helium." Separation Science. Vol. 2.(1967) Page 555.

(37) Hwang, S. T. "Interaction Energy in Surface Diffusion." A.I.Ch.E. Symposium on Recent Advances in Separation Processes. (1968).

(38) JuHola, A. J. Div. 10, NURC Formal Report. (1945).

(39) Kammermeyer, K. "Vapor Transfer Through Barriers." Ind. Eng. Chem. Vol. 50. (1958) Page 697.

(40) Kammermeyer, K., Wyrick. Ind. Eng. Chem. Vol. 50. (1958) Page 1309.

(41) McGlasnan, M. L., Potter, D. J. B. "The Second Virial Coefficients of Some N-Alkanes." Proc. Joint Conf. Thermodynamics and Transport Properties of Fluids. Inst. Mech. E. (1958) Page 60.

(42) Peterson, D. L., Redlich, O. "Sorption of Normal Paraffins by Molecular Sieves Type 5A." J. Chem. Eng. Data. Vol. 1. (1962) Page 570.

(43) Reid, R. C., Sherwood, T. K. The Properties of Gases and Liquids. 2nd Ed. New York: McGraw-Hill Book Co., 1966.

(44) Rivarola, J. B., Smith, J. M. "Surface Diffusion of Carbon Dioxide on Alumina." I. & E. C. Fund. Vol. 3. (1964) Page 308.

(45) Ross, S., Oliver, J. P. On Physical Adsorption. New York: Interscience Publishers, 1964.

(46) Rothfeld, L. B. "Gaseous Counterdiffusion in Catalysis Pellets." A.I.Ch.E. J. Vol. 9. (1963) Page 19.

(47) Sakashita, K., Arai, Kobayashi. "Surface Diffusion in Porous Solids." Chem. Eng. (Japan). Vol. 31. (1967) Page 920.

(48) Satterfield, C. N., Iino, H. "Surface Diffusion of Chemisorped Hydrogen on Nickel" Private Manuscript. 1967.

(49) Scott, D. S., Dullien, F. A. L. A.I.Ch.E. J. Vol. 8. (1962) Page 293.

(50) Sips, R. "On the Structure of a Catalyst Surface." J. Chem. Phys. Vol. 16. (1948) Page 490.

(51) Sobolev, I., Meyer, J. A., Stannett, V., Szwarc, M. "Permeation, Diffusion, and Solubility of Methyl Bromide and Isobutene in Polyethylene." Ind. Eng. Chem. Vol. 49. (1957) Page 441.

(52) Toth, J. "Evaluation of Activated Charcoal Used in Gasoline Technology on the Basis of a New Adsorption Theory." Hungarian Acad. Sci. Oil Sci. Sess., Budapest, 1962. Translation TR-63-19.

(53) Waack, R., Alex, N. H., Frisch, H. L., Stannett, V., Szwarc, M. "Permeability of Polymer Films to Gases and Vapors." Ind. Eng. Chem. Vol. 47. (1955) Page 2524.

(54) Wakao, N., Smith, J. M. "Diffusion in Catalysis Pellets." Chem. Eng. Sci. Vol. 17. (1962) Page 825.

(55) Wakao, N., Otani, S., Smith, J. M. "Significance of Pressure Gradients in Porous Material. I. Diffusion and Flow in Fine Capillarys." A.I.Ch.E. J. Vol. 11. (1965) Page 435.

(56) Wicke, E., Brotz, W. Chem. Ing.-Technik. Vol. 21. (1949) Page 219.

(57) Wilke, E., Kallenback, R. Kolloid Z. Vol. 97. (1941) Page 135.

(58) Wilke, C. R., Lee, C. Y. "Estimation of Diffusion Coefficients for Gases and Vapors." Ind. Eng. Chem. Vol. 47. (1955) Page 1253.

APPENDIX A

FLOWMETER CALIBRATION

The capillary flow meters used to measure the inlet gas flow were calibrated using a bubble flowmeter. The results were correlated using a Hagen-Poiseuille Equation modified for gaseous flow.

The form of the Hagen-Poiseuille Equation modified was

$$W = \frac{\pi \Delta P \ \bar{r}_c^{\,4}}{8 \mu L \ Z} \tag{43}$$

At the relatively low pressures used, it is assumed that the compressibility is constant, and therefore, the molar density is directly proportional to pressure and inversely proportional to temperature. It is also assumed that the capillary radius, $\bar{r}_c$, and length, L, are constant. The viscosities of the gases were referenced to a temperature of 24^{o} C. Variation from this temperature was compensated for by the use of the square root of the ratio of absolute temperature to that of the reference temperature, as predicted by the theory of gases composed of hard spheres. The resultant form of the Hagen-Poiseuille Equation used is

$$W = K \frac{\bar{P} \ \Delta P}{T \quad (T/T_R)^{1/2}} \tag{44}$$

where K is the proportionality constant to be determined experimentally.

The molar densities used to convert the bubble meter volumetric flow rates to molar flow rates, were calculated for helium, nitrogen and methane using the ideal gas law, and for propane using a Second Virial Coefficient Equation of State (41).

Meter A

Methane	$K = 1.2792 \times 10^{-6}$
Helium	$K = 0.4328 \times 10^{-6}$

Meter B

Propane	$K = 1.8553 \times 10^{-6}$
Nitrogen	$K = 0.5515 \times 10^{-6}$

TABLE XVI

METHANE

Flowmeter Data

$\overline{W}$ $\left(\frac{c.c.}{min.}\right)$	$W \times 10^3$ $\left(\frac{moles}{min.}\right)$	$\overline{P}$ (mm Hg)	ΔP (mm T.E.G.)	T (^oK)	$\left[\frac{\overline{P}\ \Delta P}{T(T/T_R)^{1/2}}\right] \times 10^{-3}$
5.88	0.2381	755.40	120.14	296.0	3.065
22.14	0.9058	782.07	427.99	294.0	1.1645
21.43	0.8675	782.32	415.04	294.0	1.1239
23.91	0.9774	782.83	462.03	294.0	1.2594
16.18	0.6847	774.45	333.50	295.0	0.8903
25.99	1.0516	778.26	516.13	295.5	1.3593
21.43	0.8655	774.45	426.21	295.5	1.1232
32.07	1.2884	787.65	615.95	295.5	1.6832
14.39	0.5795	763.78	284.48	296.0	0.7432
6.83	0.2739	748.79	140.72	296.0	0.3574
6.35	0.2565	752.35	128.78	296.0	0.3284
6.32	0.2559	752.09	129.29	295.0	0.3310
21.23	0.8617	773.18	414.78	295.0	1.1045

TABLE XVI (Continued)

$\overline{W}$ $\left(\frac{\text{c.c.}}{\text{min.}}\right)$	$W \times 10^3$ $\left(\frac{\text{moles}}{\text{min.}}\right)$	$\overline{P}$ (mm Hg)	ΔP (mm T.E.G.)	T (^oK)	$\left[\frac{\overline{P}\ \Delta P}{T(T/T_R)^{1/2}}\right] \times 10^{-3}$
35.86	1.4513	794.00	679.70	295.0	1.8826
33.21	1.3445	791.21	632.71	295.0	1.7464
22.99	0.9290	778.00	448.82	296.0	1.2013
26.83	1.0833	782.57	521.21	296.0	1.4058
29.27	1.1774	783.08	569.47	296.0	1.5387
29.61	1.1512	776.22	572.26	303.0	1.4839
31.06	1.2051	782.07	596.90	303.5	1.5619
31.23	1.2090	780.80	600.71	304.0	1.5664
31.25	1.2562	787.91	594.11	296.0	1.6226
32.73	1.3173	790.96	624.33	296.0	1.7116
2.45	0.0987	751.08	51.05	296.5	0.1284

$K = 0.7726 \times 10^{-6}$

TABLE XVII

PROPANE

Flowmeter Data

$\overline{W}$ $\left(\frac{c.c.}{min.}\right)$	$W \times 10^3$ $\left(\frac{moles}{min.}\right)$	$\overline{P}$ (mm Hg)	ΔP (mm T.E.G.)	T (^oK)	$\left[\frac{\overline{P}\ \Delta P}{T(T/T_R)^{1/2}}\right] \times 10^{-3}$
37.34	1.6385	790.96	518.41	294.0	1.3948
29.56	1.2637	781.30	412.24	294.5	1.0935
33.46	1.4548	784.61	464.82	294.5	1.2381
25.28	1.0868	775.97	354.56	294.5	0.9342
18.75	0.7969	767.33	263.65	294.5	0.6871
13.96	0.6001	756.92	199.39	294.5	0.5123
26.47	1.1313	776.22	373.89	296.0	0.9806
19.38	0.8186	768.55	276.10	296.0	0.7168
7.08	0.2938	752.86	103.12	296.0	0.2626

$K = 1.1571 \times 10^{-6}$

TABLE XVIII

HELIUM

Flowmeter Data

$\overline{W}$ $\left(\frac{c.c.}{min.}\right)$	$W \times 10^3$ $\left(\frac{moles}{min.}\right)$	$\overline{P}$ (mm Hg)	ΔP (mm T.E.G.)	T (^oK)	$\left[\frac{\overline{P}\ \Delta P}{T(T/T_R)^{1/2}}\right] \times 10^{-3}$
24.55	0.9846	1013.18	655.20	296.5	2.2389
20.03	0.8034	1030.37	530.35	296.5	1.8430
14.57	0.5844	1041.16	377.60	296.5	1.3259
4.13	0.1659	1067.02	109.15	296.5	0.3928
18.92	0.7608	1031.16	495.75	296.5	1.7241
21.52	0.8538	943.03	646.95	297.2	2.0528
13.94	0.5510	993.02	387.05	297.2	1.2932

$K = 0.4328 \times 10^{-6}$

TABLE XIX

NITROGEN

Flowmeter Data

$\overline{W}$ $\left(\frac{c.c.}{min.}\right)$	$W \times 10^3$ $\left(\frac{moles}{min.}\right)$	$\overline{P}$ (mm Hg)	ΔP (mm T.E.G.)	T (^oK)	$\frac{\overline{P}\ \Delta P}{T(T/T_R)^{1/2}} \times 10^{-3}$
32.16	1.4069	1384.0	546.53	297.2	2.5452
23.99	1.0482	1379.0	411.15	297.2	1.9077
17.03	0.7437	1382.9	290.40	297.2	1.3513
11.34	0.4950	1382.8	192.20	297.2	0.8943

$K = 0.5515 \times 10^{-6}$

APPENDIX B

GAS CHROMATOGRAPH CALIBRATION

The gas chromatograph used to analyze the composition of the diffusion cell outlet gases was calibrated by plotting the partial pressure of pure gases versus the peak height of the response.

The pressure of pure gas in the gas chromatograph sampling valves was measured by a Texas Instruments Precision Pressure Gauge with a Quartz Bourdon-Tube capsule with an estimated accuracy of $\pm$0.005 p.s.i.a. A constant volume sample was then injected into the chromatograph and the peak height of the response was measured. The chromatograph response was indicated on a Honeywell Gas Chromatograph Recorder with an estimated accuracy of $\pm$0.2% of full scale. In the low pressure range used, up to 3.0 p.s.i.a., the response was found to be a linear function of pressure.

The ratios of attenuation responses were measured by sampling a gas at a nearly constant pressure and measuring the response using successively higher attenuations. The ratios of peak height over pressure at the attenuations were compared to give the ratio of attenuation responses.

For calculation of composition of mixtures, it was assumed that the response of each component in a mixture is independent of other components when the response peaks are completely separated.

TABLE XX

TYPICAL GAS CHROMATOGRAPH CALIBRATION

Helium and Nitrogen

Helium			Nitrogen		
Pressure (psia)	Peak Height (50=Full Scale)	Attenuation	Pressure (psia)	Peak Height (50=Full Scale)	Attenuation
		Column 1			
2.495	42.0	8	2.457	49.7	32
2.498	42.1	8	2.160	44.1	32
2.498	42.1	8	2.161	44.0	32
2.076	35.3	8	1.849	37.4	32
1.874	32.1	8	1.602	32.9	32
1.698	28.9	8	1.440	29.1	32
1.287	21.9	8	1.240	25.1	32
0.996	17.1	8	0.976	19.6	32

TABLE XX (Continued)

Helium			Nitrogen		
Pressure (psia)	Peak Height (50=Full Scale)	Attenuation	Pressure (psia)	Peak Height (50=Full Scale)	Attenuation
		Column 2			
2.196	37.3	4	2.275	41.1	16
2.218	37.6	4	2.293	41.1	16
1.948	33.5	4	2.122	37.9	16
1.770	30.3	4	1.844	33.0	16
1.595	27.3	4	1.701	30.2	16
1.424	24.8	4	1.585	26.4	16
1.254	21.6	4	1.339	23.3	16
1.005	17.5	4	1.151	20.3	16

Columns 12 ft.-1/4 in. "Porapak Type Q", 50-80 Mesh.
Column Temperature 45° C.
H_2 Carrier Gas Pressure 33 p.s.i.g.
Carrier Gas Flow Rate: 80 cc/min. H_2.

TABLE XXI

RATIO OF ATTENUATIONS

Data

Attenuation	Pressure	Peak Height	$\frac{\text{Peak Height}}{\text{Pressure}}$	Gas
32	1.689	8.6	5.09	Air
32	1.679	9.2	5.48	Air
16	1.713	19.4	11.33	Air
16	1.704	19.7	11.56	Air
8	1.687	39.4	23.36	Air
8	1.720	40.1	23.31	Air
8	0.526	11.8	22.43	Air
8	0.526	11.7	22.24	Air
4	0.526	24.4	46.39	Air
4	0.526	24.5	46.58	Air
2	0.522	48.9	93.68	Air
2	0.526	49.4	93.92	Air
4	0.584	10.3	17.64	He
4	0.585	10.3	17.61	He
2	0.583	21.9	37.56	He
2	0.583	21.9	37.56	He
1	0.581	44.9	77.28	He
1	0.596	46.0	77.18	He

TABLE XXII

RATIO OF ATTENUATIONS

Results

$$\left[\frac{\text{Peak Height}}{\text{Pressure}}\right]_{32} \Big/ \left[\frac{\text{Peak Height}}{\text{Pressure}}\right]_{8} = 0.226$$

$$\left[\frac{\text{Peak Height}}{\text{Pressure}}\right]_{16} \Big/ \left[\frac{\text{Peak Height}}{\text{Pressure}}\right]_{8} = 0.490$$

$$\left[\frac{\text{Peak Height}}{\text{Pressure}}\right]_{8} \Big/ \left[\frac{\text{Peak Height}}{\text{Pressure}}\right]_{8} = 1.00$$

$$\left[\frac{\text{Peak Height}}{\text{Pressure}}\right]_{4} \Big/ \left[\frac{\text{Peak Height}}{\text{Pressure}}\right]_{8} = 2.08$$

$$\left[\frac{\text{Peak Height}}{\text{Pressure}}\right]_{2} \Big/ \left[\frac{\text{Peak Height}}{\text{Pressure}}\right]_{8} = 4.44$$

$$\left[\frac{\text{Peak Height}}{\text{Pressure}}\right]_{1} \Big/ \left[\frac{\text{Peak Height}}{\text{Pressure}}\right]_{8} = 9.12$$

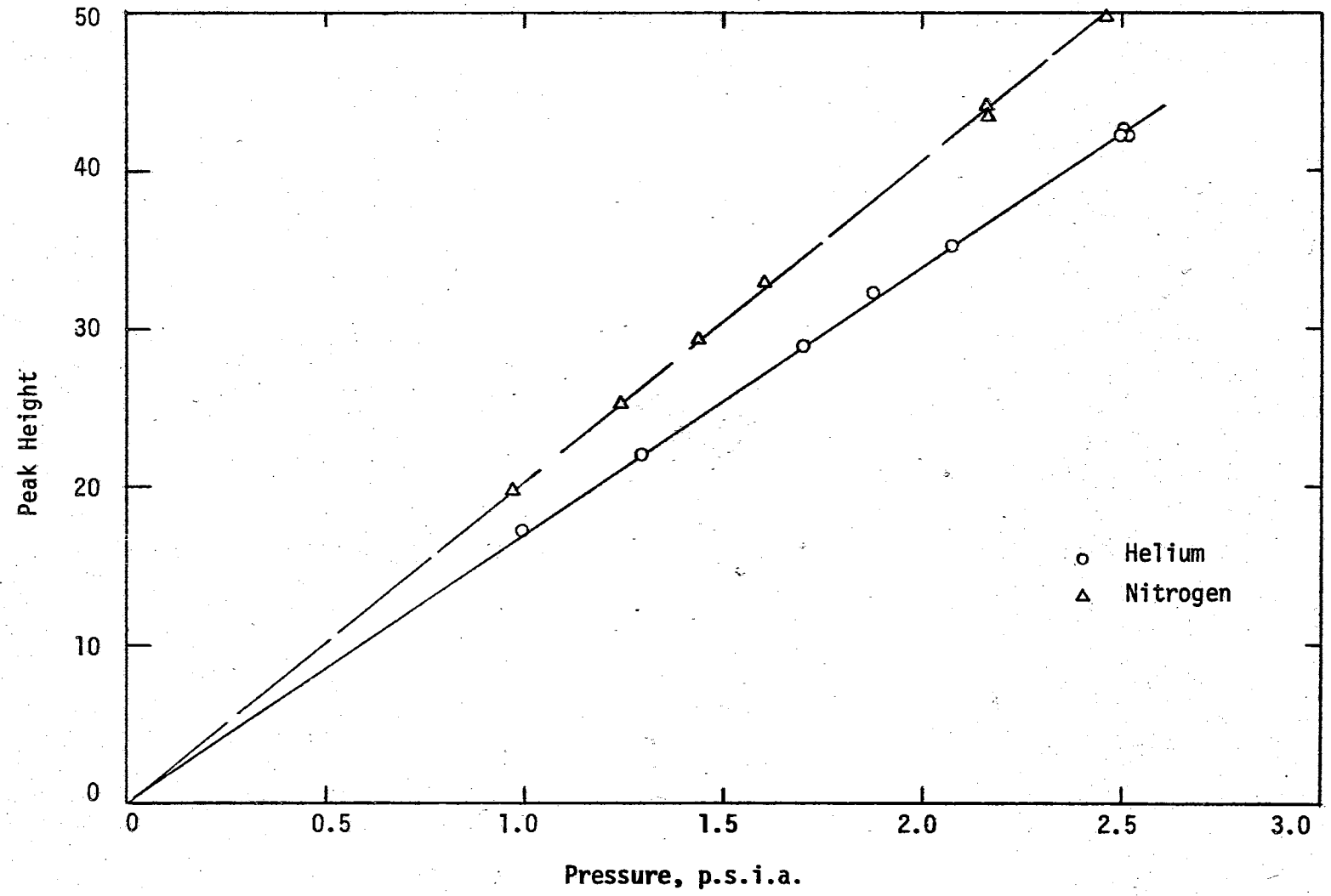

Figure 8. Gas Chromatograph Calibration -- Helium-Nitrogen, Column 1

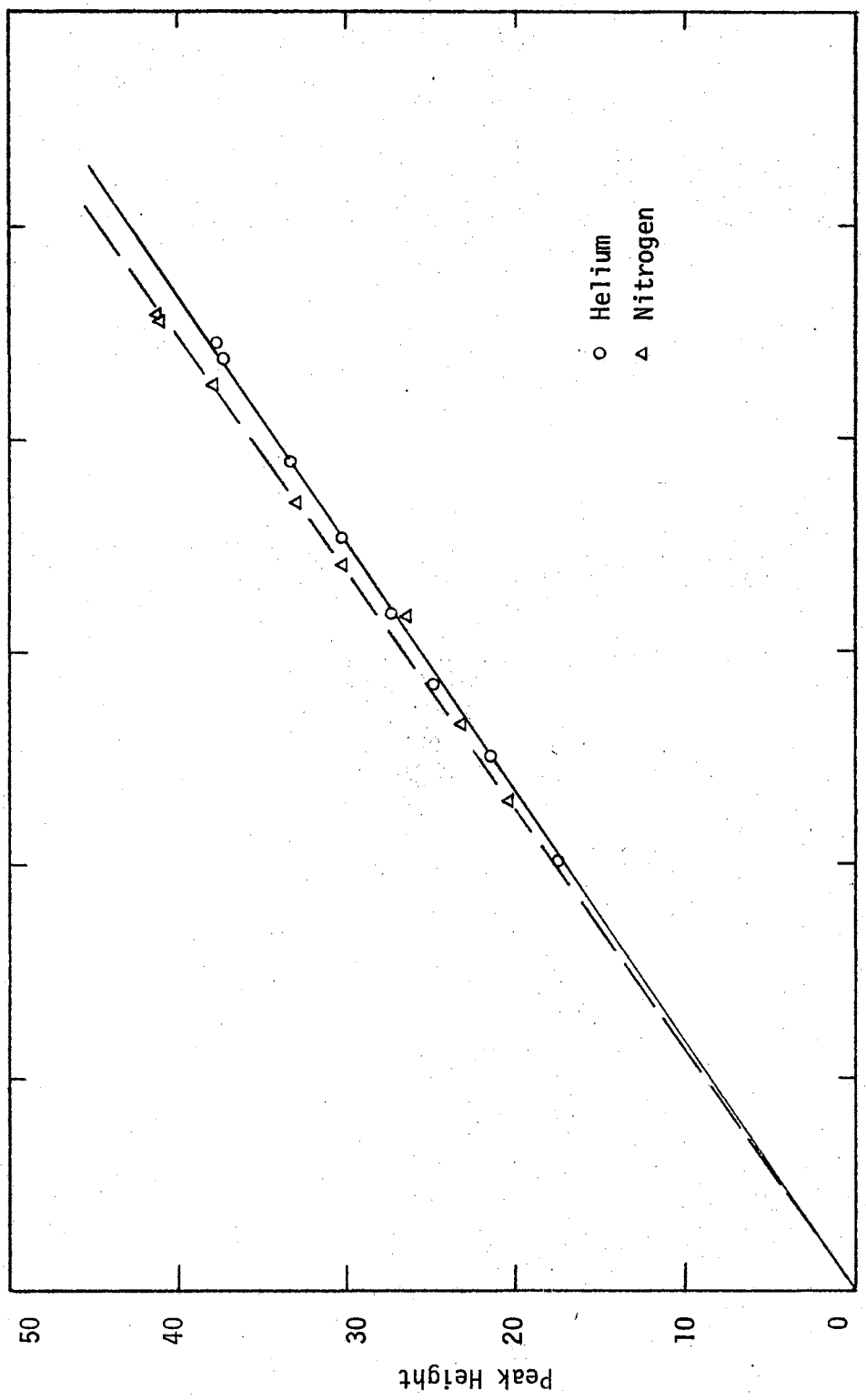

Figure 9. Gas Chromatograph Calibration -- Helium-Nitrogen, Column 2

APPENDIX C

ADSORPTION DATA

The adsorption data of methane and propane on Columbia Carbon NXC activated carbon was furnished by Continental Oil Company (17) and is used here with their permission. The data is shown on Tables XXIII and XXIV. The adsorption isotherms for methane and propane on activated carbon appear to fit Brunauer's (12, 13) classification of Type I isotherms.

In the pressure range up to 1 atm., the methane isotherm is adequately represented by Henry's Law

$$\overline{C}_A' = H P_A \tag{45}$$

The Langmuir adsorption isotherm equation

$$\overline{C}_A' = \frac{A_m b P_A}{1 + b P_A} \tag{46}$$

is fitted to the data for propane.

The Langmuir adsorption model has the following implicit assumptions, as listed by Ross and Oliver (45):

(a) gaseous adsorption is an ideal gas,

(b) adsorption is in a monomolecular layer,

(c) no adsorbent-adsorbate interaction,

(d) adsorption is localized, i.e., occurs at definite points,

(e) all adsorption sites are equal.

A key assumption in the derivation of Equation (46) is each pore or site at which adsorption takes place tends to adsorb or desorb equally under the same conditions. This appears to be far from true (19). Several modified forms of the Langmuir equation have been suggested (50, 52, 42) to account for this inhomogeneity. The Langmuir model is chosen for its simplicity and is found to fit the data adequately. The coefficients are

$$A_m = 4.45 \text{ g-mole/cm}^2$$

$$b = 0.315 \text{ psia}^{-1}$$

The values used in the diffusion equation are then

$$K(P_A) = \frac{A_m\, b}{1 + b\, P_A} \tag{47}$$

and

$$\frac{\partial K(P_A)}{\partial P_A} = \frac{-A_m\, b^2}{(1 + b\, P_A)^2} \tag{48}$$

TABLE XXIII

PROPANE ADSORPTION DATA

Columbia Carbon NXC Activated Carbon

Temperature 77° F

Pressure (psia)	$\overline{C'}$ X 10^{10} (g moles/cm^2)	$\overline{C'}$ Langmuir X 10^{10} (g moles/cm^2)
0.15	0.1644	0.222
0.16	0.1682	0.237
0.62	1.033	0.794
0.67	0.9691	0.846
2.19	2.059	1.93
6.06	2.970	3.02
16.53	3.767	3.79
29.63	4.041	4.05
58.63	4.315	4.24
99.93	4.421	4.32

TABLE XXIV

METHANE ADSORPTION DATA

Columbia Carbon NXC Activated Carbon

Temperature 77° F

Pressure (psia)	$\overline{C}'$ X 10^{10} (g moles/cm^2)	$\overline{C}'$ Henry's Law X 10^{10} (g moles/cm^2)
2.4	0.2233	0.159
4.6	0.3842	0.406
21.0	1.163	1.389
56.5	1.978	-
88.5	2.534	-
102.5	2.674	-
177	3.401	-
204	3.478	-
262	3.790	-
277	3.920	-
314	4.180	-
367	4.283	-
432	4.257	-

$H = 0.661 \times 10^{-11}$, g moles cm^{-2} $psia^{-1}$

$K_S = \frac{H}{RT} = 0.270 \times 10^{-5}$ cm^{-1}

APPENDIX D

SAMPLE CALCULATION

The calculation of flux rates and effective diffusivities from the experimental data was done by making a material balance around the cell and defining an effective diffusivity as if the pellet is an open space in the mounted brass disk. The outlet gases are assumed to be the concentration at the pellet face.

The Fick's Law diffusion coefficient, D_{A-B}, was estimated by Fuller, Schettler and Giddings (43) method, when a value was not found in the literature. The Knudsen diffusion coefficient was estimated using Equations (2), (3), (4), and $K_o = 2/3$.

Two programs were written to aid in the calculations. The first converts the experimental results of Tables I, II and III to those values reported in Tables IV, V and VI. It was written for an IBM Model 1620 computer equipped with a disk memory unit. The second program calculates the predicted gas phase fluxes according to the Wakao and Smith model. It was written for an IBM Model 7040 computer.

TABLE XXV

EXPERIMENTAL DATA PROCESSOR

```
ZZFOR
*LDISKKELLYA
C      TOM KELLY       DATA PROCESSOR
       DIMENSION PHPSC(2,2),RATTN(65),IATNR(2,2),PHR(20,2,2),PRSR(20,2,2)
      1,PCTR(20,2,2),PCTA( 9,2,2),PCELL(20),PMTA(20),ANA(20),ANB(20),TABS
      2(20),IATNC(2,2)
       COMMON  PCELL,PMTA,ANA,ANB,DIAM,DELTA,TABS,PCTR,N
       READ 101,N
       READ 100,((IATNC(I,J),PHPSC(I,J),J=1,2),I=1,2)
C    RATIO OF ATTENUATIONS
       RATTN(1)=9.121
       RATTN(2)=4.199
       RATTN(4)=2.081
       RATTN(8)=1.0
       RATTN(16)=0.4901
       RATTN(32)=0.226
C
C   CALCULATION OF COMPOSITIONS
       DO 30 NN=1,N
       DO 30 I=1,2
       DO 3 K=1,6
       PHR(K,I,1)=0.0
     3 PHR(K,I,2)=0.0
       PCTR(NN,I,2)=0.0
       PCTR(NN,I,1)=0.0
       READ 105,IATNR(I,1),IATNR(I,2),(PHR(K,I,1),PHR(K,I,2),K=1,6)
       DO 5 K=1,6
       IF (PHR(K,I,1))4,4,5
     4 KK=K-1
       GO TO 6
     5 CONTINUE
     6 CONTINUE
       DO 30 K=1,KK
       DO 20 J=1,2
       IIA=IATNC(I,J)
       IIB=IATNR(I,J)
       CPHR=PHR(K,I,J)*(RATTN(IIA)/RATTN(IIB))
    20 PRSR(K,I,J)=CPHR/PHPSC(I,J)
       TPRSR=PRSR(K,I,1)+PRSR(K,I,2)
       PCTA(K,I,1)=PRSR(K,I,1)/TPRSR
       PCTA(K,I,2)=PRSR(K,I,2)/TPRSR
       AK=KK
       PCTR(NN,I,2)=PCTR(NN,I,2)+PCTA(K,I,2)/AK
       PCTR(NN,I,1)=PCTR(NN,I,1)+PCTA(K,I,1)/AK
    30 CONTINUE
       PUNCH 150,((PCTR(NN,I,1),PCTR(NN,I,2),NN,I,I=1,2),NN=1,N)
       CALL LINK(KELLYB)
   100 FORMAT (4(I2,F8.6))
   101 FORMAT (I3)
   105 FORMAT(2I2,12F4.2)
   150 FORMAT (18HMOLE FRACTION 1 = ,F6.4,3X,18HMOLE FRACTION 2 = ,F6.4,3
      1X,4HNN= ,I3,6HVALVE ,I3)
       END
ZZFOR
*LDISKKELLYB
       DIMENSION TEG(20,2),HG(20,2),TEMP(20),PATM(20),PCHG(20),FMC(2),FRT(AZ
      1(20,2)
       DIMENSION PCELL(20),PMTA(20),ANA(20),ANB(20),TABS(20),PCTR(20,2,2)
       COMMON  PCELL,PMTA,ANA,ANB,DIAM,DELTA,TABS,PCTR,N
C   CALCULATION OF FLOW RATES
       READ 112,FMC(1),FMC(2)
       FMC(1)=FMC(1)/60.0
```

TABLE XXV (Continued)

```
      FMC(2)=FMC(2)/60.0
      READ 111,((TEG(NN,I),HG(NN,I),I=1,2),TEMP(NN),PATM(NN),PCHG(NN),NN
     1=1,N)
      DO 40 NN=1,N
      DO 40I=1,2
      PBAR=PATM(NN)+HG(NN,I)-0.5*TEG(NN,I)*0.08307
      TABS(NN)=TEMP(NN)+273.2
      AVAR=PBAR*TEG(NN,I)/(TABS(NN)*(TABS(NN)/297.2)**0.5)
   40 FRT(NN,I)=AVAR*FMC(I)
      READ 120,DELTA,DIAM
      AREA=3.1416*(DIAM**2)/4.0
      DO 50NN=1,N
      ANAT=FRT(NN,1)*PCTR(NN,1,2)*PCTR(NN,2,1)-FRT(NN,2)*PCTR(NN,1,1)*PC
     1TR(NN,2,1)
      ANBT=FRT(NN,2)*PCTR(NN,2,1)*PCTR(NN,1,2)-FRT(NN,1)*PCTR(NN,2,2)*PC
     1TR(NN,1,2)
      ANAB=PCTR(NN,1,2)*PCTR(NN,2,1)-PCTR(NN,1,1)*PCTR(NN,2,2)
      ANA(NN)=ANAT/(ANAB*AREA)
      ANB(NN)=ANBT/(ANAB*AREA)
      RNANB=ANA(NN)/ANB(NN)
      PUNCH 162,ANA(NN),ANB(NN),RNANB,NN
      PCELL(NN)=-PCHG(NN)+PATM(NN)
      PMTA(NN)=PCELL(NN)*0.0013158
   50 CONTINUE
      PUNCH 161,(FRT(NN,1),FRT(NN,2),NN,NN=1,N)
      CALL LINK(KELLYC)
  111 FORMAT (7F5.2)
  112 FORMAT (2F15.10)
  120 FORMAT (2F10.5)
  161 FORMAT (2E15.10,I2)
  162 FORMAT (3(E15.10,2X),I2)
      END
ZZFOR
*LDISKKELLYC
      DIMENSION PCELL(20),PMTA(20),ANA(20),ANB(20),TABS(20),PCTR(20,2,2)
      DIMENSION DAB(20),PDAB(20),DE(20),PDE(20)
      COMMON  PCELL,PMTA,ANA,ANB,DIAM,DELTA,TABS,PCTR,N
C  CALCULATION OF DAB ASSUMING AN OPEN ORIFICE
  200 CONTINUE
      READ 172,ICNTOP,ICNBOT
      DO 60 NN=1,N
C
      RRR=0.0
      JJJ=0
      GO TO (51,52,53,54,55),ICNTOP
   58 GO TO (57,59),JJJ
   57 GO TO (51,52,53,54,55),ICNBOT
C                    METHANE       CN=1
   51 PC=99.3
      VC=45.8
      TC=190.7
      BA=1.345*(TC/TABS(NN))**2
      B=-VC*(0.145-BA)
      RHO=(-1.0+(1.0+(4.0*B*PMTA(NN))/(82.05*TABS(NN)))**0.5)/(2.0*B)
      RRR=RRR+RHO
      JJJ=JJJ+1
      GO TO 58
C                  GOOF UP           CN=2
   52 TYPE 173
      PAUSE
      JJJ=JJJ+1
      GO TO 58
```

TABLE XXV (Continued)

```
C                    PROPANE        CN=3
   53 PC=200.0
      VC=42.0
      TC=370.0
      BA=1.345*(TC/TABS(NN))**2
      BB=0.0057*(2.0**1.5)*((TC/TABS(NN))**6)
      B=-VC*(0.145-BA-BB)
      RHO=(-1.0+(1.0+(4.0*B*PMTA(NN))/(82.05*TABS(NN)))**0.5)/(2.0*B)
      RRR=RRR+RHO
      JJJ=JJJ+1
      GO TO 58
C           BUTANE              CN=4
   54 PC=255.0
      VC=37.5
      TC=425.2
      BA=1.345*(TC/TABS(NN))**2
      BB=0.0057*(3.0**1.5)*((TC/TABS(NN))**6)
      RHO=(-1.0+(1.0+(4.0*B*PMTA(NN))/(82.05*TABS(NN)))**0.5)/(2.0*B)
      RRR=RRR+RHO
      JJJ=JJJ+1
      GO TO 58
C          HELIUM OR NITROGEN     CN=5
   55 RHO=PMTA(NN)/(82.05*TABS(NN))
      RRR=RRR+RHO
      JJJ=JJJ+1
      GO TO 58
C
   59 TOTN=ANA(NN)-ANB(NN)
      RHO=RRR/2.0
      C1=PCTR(NN,1,1)-ANA(NN)/TOTN
      DABT=TOTN*DELTA/RHO
      DABB=LOGF((PCTR(NN,2,1)-(ANA(NN)/TOTN))/C1)
      DAB(NN)=DABT/DABB
      PDAB(NN)=DAB(NN)*PCELL(NN)
      PUNCH 171,DAB(NN),PDAB(NN),PCELL(NN),NN
   60 CONTINUE
  171 FORMAT(3(E15.10,2X),I2)
  172 FORMAT (2I2)
  173 FORMAT (7HGOOF UP)
  175 FORMAT(3(F5.4,2X),F3.1)
  176 FORMAT (2F4.4)
  180 FORMAT(I2,F5.4)
      END
```

TABLE XXVI

WAKAO AND SMITH COMPUTER PROGRAM

```
C     WAKAO AND SMITH MODEL FOR GAS DIFFUSION IN POROUS SOLIDS
      DIMENSION PCELL( 6),PMTA( 6),ANA( 6),ANB( 6),TABS( 6),PCTR( 6,2,2)
      DIMENSION DBA( 6),PDAB( 6),DE( 6),PDE( 6)
      DIMENSION T(6),P(6),YA1(6),YA2(6),YB1(6),YB2(6),DKKAA(6),DKKAI(6),
     1DKDAA(6),DKDAI(6),DKKBA(6),DKKBI(6),DKDBA(6),DKDBI(6),DAB(6),ALPHA
     1(3),ALPHAB(4,3)
      DIMENSION DKA(6),DKI(6),Y1(6),Y2(6),FXAMAE(6),FXAMIE(6),FXASEE(6),
     1FXATOE(6),FXAMIS(6),FXASES(6),FXATOS (6),FLXTOE(4,3,6),FLXMAE(4,3,
     16),FLXMIE(4,3,6),FLXSEE(4,3,6),FLXTOS(4,3,6),FLXMAS(4,3,6),FLXMIS(
     34,3,6),FLXSES(4,3,6)
      DIMENSION ALPCLE(4,3,6),FLSMAW(4,6),ALPCLS(4,3,6),FLSMIW(4,6),FLSS
     1EW(4,6),FLSTOW(4,6),TITLE(12)
      REAL KS
C           T. J. KELLY
      FLMAMI(A,B,C,D,E,F)=(F**2.0)*ALOG((1.0-(A*C)+(D/E))/(1.0-A*B+D/E))
      FLSESF(A,B,C,D,F)=4.0*EA*(1.0-EA)*A*(B-C)/((1.0+G)*(1.0-A*(B+C)/2.
     10+(D/F)/(1.0+1.0/G)))
      FAC(D,E,F)=D*(G+F/E)/(F*(1.0+G))
      FLSREF(A,B,C,D,E,F)= 4.0*EA*(1.0-EA)*(ALOG((1.0-A*C+FAC(D,E,F))/(1
     1.0-A*B+FAC(D,E,F))))/(1.0+G)
      FLMISF(A,B,C,D,F)=(EI**2)*A*(B-C)/(1.0-A*((B+C)/2.0)+(D/F))
      VEL(A,B)=(21.174E07*A/B)**0.5
      FLAX(A,H,D,W,V)=H*W*D/(R*V*AL*A)
C     A=ALPHA  B=Y1  C=Y2  D=DAB  E=DK OR DKA  F=DKI OR EI OR EA  H=FLUX
C     W=P  V=T  G=CONSTANT
  300 CONTINUE
      PRINT 99
   99 FORMAT(1H1)
      READ  103,(TITLE(I),I=1,12)
  103 FORMAT(12A6)
      PRINT 104,(TITLE(I),I=1,12)
  104 FORMAT(///,20X,12A6)
   10 READ 100,EA,EI,AA,AI,AL
  100 FORMAT(5F10.5)
      AA=AA*(10.0**(-8.0))
      AI=AI*(10.0**(-8.0))
      READ 102,R,DS,KS,AM,BM,DABO,SUMDVA,SUMDVB
  102 FORMAT(8F10.5)
      G=((1.0-EA)**2.0)/EI**2.0
    9 DO 20I=1,6
      READ 101,T(I),P(I),YA1(I),YA2(I)
  101 FORMAT(4F10.5)
      YB1(I)=1.0-YA1(I)
      YB2(I)=1.0-YA2(I)
C     KNUDSEN
C     CALCULATION OF DIFFUSSION COEFFICIENTS A
      DKKAA(I)=2.0*VEL(T(I),AM)*AA/3.0
      DKKAI(I)=DKKAA(I)*AI/AA
      DKDAA(I)=DKKAA(I)*9.0/13.0
      DKDAI(I)=DKDAA(I)*AI/AA
C     DIFFUSSION COEFICIENTS B
      DKKBA(I)=2.0*VEL(T(I),BM)*AA/3.0
      DKKBI(I)=DKKBA(I)*AI/AA
      DKDBA(I)=DKKBA(I)*9.0/13.0
      DKDBI(I)=DKDBA(I)*AI/AA
C     BULK
      DABFSG=0.00100*(T(I)**1.75)*((1.0/AM+1.0/BM)**0.5)/(P(I)*(SUMDVA**
     10.3333+SUMDVB**0.3333)**2.0)
      IF(DABO)7,7,8
    7 DABO=0.00100*(298.0 **1.75)*((1.0/AM+1.0/BM)**0.5)/(      (SUMDVA**
     10.3333+SUMDVB**0.3333)**2.0)
    8 DAB(I)=DABO*((T(I)/298.0)**1.75)/P(I)
```

TABLE XXVI (Continued)

```
      PRINT 260,DAB(I),DABFSG,I
  260 FORMAT(5X,4HDAB=,E12.6,5X,7HDABSFG=,E12.6,5X,4HNO.=,I2)
   20 CONTINUE
      PRINT 220,EA,EI,AA,AI,AL
  220 FORMAT (30X,21HWAKAO AND SMITH MODEL/35X,9H          ,//20X,4HEA= ,
     1F10.5,10X,4HEI= ,F10.5,/20X,14HRADIUS MACRO =,E12.6,10X,14HRADIUS
     1MICRO =,E12.6,/20X,15HLENGH OF PELLFT,F10.5,/20X,17HDIMENSIONS IN
     3CM.)
      PRINT 221
  221 FORMAT(3X,3HNO.10X,4HTEMP,7X,5HPRESS,9X,3HYA1,9X,3HYA2)
      PRINT 222,(I,T(I),P(I),YA1(I),YA2(I),I=1,6)
  222 FORMAT(4X,I2,2X,4F12.6)
      PRINT 200
  200 FORMAT(///3X,3HNO.10X,10HDKA NORMAL,15X,8HDKA DEF.,/13X,5HMACRO,7X
     1,5HMICRO,7X,5HMACRO,7X,5HMICRO/)
      PRINT 201,(I,DKKAA(I),DKKAI(I),DKDAA(I),DKDAI(I),I=1,6)
  201 FORMAT(4X,I2,4E12.6)
      PRINT 202
  202 FORMAT(///3X,3HNO.10X,10HDKB NORMAL,15X,8HDKB DEF.,/13X,5HMACRO,7X
     1,5HMICRO,7X,5HMACRO,7X,5HMICRO/)
      PRINT 203,(I,DKKBA(I),DKKBI(I),DKDBA(I),DKDBI(I),I=1,6)
  203 FORMAT(4X,I2,4E12.6)
      NNN=1
   69 GO TO (60,62,64,66,68),NNN
   60 DO 61 J=1,6
      DKA(J)=DKKAA(J)
      DKI(J)=DKKAI(J)
      Y1(J)=YA1(J)
   61 Y2(J)=YA2(J)
      DIREC=1.0
      ALPHAB(1,2)=1.0-(AM/BM)**0.5
      GO TO 35
   62 DO 63 J=1,6
      DKA(J)=DKDAA(J)
   63 DKI(J)=DKDAI(J)
      ALPHAB(2,2)=ALPHAB(1,2)
      GO TO 35
   64 DO 65 J=1,6
      DKA(J)=DKKBA(J)
      DKI(J)=DKKBI(J)
      Y1(J)=YB1(J)
   65 Y2(J)=YB2(J)
      ALPHAB(3,2)=1.0-(BM/AM)**0.5
      GO TO 35
   66 DO 67 J=1,6
      DKA(J)=DKDBA(J)
   67 DKI(J)=DKDBA(J)
      ALPHAB(4,2)=ALPHAB(3,2)
      GO TO 35
C     CALCULATION OF FLUXES
C     ALPHA=1.10THEO,1.00THEO,0.90THEO
C
   35 CONTINUE
      ALPHAB(NNN,1)=ALPHAB(NNN,2)*1.20
      ALPHAB(NNN,3)=ALPHAB(NNN,2)*0.80
      ALPHA(1)=ALPHAB(NNN,1)
      ALPHA(2)=ALPHAB(NNN,2)
      ALPHA(3)=ALPHAB(NNN,3)
      DO 45 I=1,3
      DO 40 J=1,6
C     EXACT EQUATION FACTORS
      FXAMAE(J)=FLMAMI(ALPHA(I),Y1(J),Y2(J),DAB(J),DKA(J),EA)*DIREC
```

TABLE XXVI (Continued)

```
      FXAMIE(J)=FLMAMI(ALPHA(I),Y1(J),Y2(J),DAB(J),DKI(J),EI)*DIREC
      FXASEE(J)=FLSREF(ALPHA(I),Y1(J),Y2(J),DAB(J),DKA(J),DKI(J))*DIREC
      FXATOE(J)=FXAMAE(J)+FXAMIE(J)+FXASEE(J)
C     SHORT EQUATION FACTORS
      FXAMIS(J)=FLMISF(ALPHA(I),Y1(J),Y2(J),DAB(J),EI)*DIREC
      FXASES(J)=FLSESF(ALPHA(I),Y1(J),Y2(J),DAB(J),DKI(J))*DIREC
      FXATOS(J)=FXAMAE(J)+FXAMIS(J)+FXASES(J)
C     EXACT EQUATION FLUXES
      FLXTOE(NNN,I,J)=FLAX(ALPHA(I),FXATOE(J),DAB(J),P(J),T(J))
      FLXMAE(NNN,I,J)=FLAX(ALPHA(I),FXAMAE(J),DAB(J),P(J),T(J))
      FLXSEE(NNN,I,J)=FLAX(ALPHA(I),FXASEE(J),DAB(J),P(J),T(J))
      FLXMIE(NNN,I,J)=FLAX(ALPHA(I),FXAMIE(J),DAB(J),P(J),T(J))
C     SHORT EQUATION FLUXES
      FLXTOS(NNN,I,J)=FLAX(ALPHA(I),FXATOS(J),DAB(J),P(J),T(J))
      FLXMIS(NNN,I,J)=FLAX(ALPHA(I),FXAMIS(J),DAB(J),P(J),T(J))
      FLXSES(NNN,I,J)=FLAX(ALPHA(I),FXASES(J),DAB(J),P(J),T(J))
      FLXMAS(NNN,I,J)=FLAX(ALPHA(I),FXAMAE(J),DAB(J),P(J),T(J))
   40 CONTINUE
      PRINT 99
      PRINT 206,ALPHA(I),NNN
  206 FORMAT(//13X,10HALPHA(I)= ,F10.6,10X,10HINDEX NNN=,I2)
      PRINT 270
  270 FORMAT(2X,3HNO.,3X,12HFACTOR MACRO,3X,12HFACTOR MICRO,2X,13HFACTOR
     2 SERIES,2X,8HEQUATION)
      DO 208J=1,6
  208 PRINT 207, J,FXAMAE(J),FXAMIE(J),FXASEE(J),FXAMAE(J),FXAMIS(J),FXA
     1SES(J)
  207 FORMAT  (3X,I2,3(5X,E10.6),5X,5HEXACT,/5X,3(5X,E10.6),5X,5HSHORT)
   45 CONTINUE
      NNN=NNN+1
      GO TO 69
   68 CONTINUE
      DO 90 J=1,6
      DO 90 I=1,3
      DO 90 NNN=1,2
      ALPCLE(NNN,I,J)=1.0+FLXTOE(NNN+2,I,J)/FLXTOE(NNN,I,J)
      ALPCLE(NNN+2,I,J)=1.0+FLXTOE(NNN,I,J)/FLXTOE(NNN+2,I,J)
      ALPCLS(NNN,I,J)=1.0+FLXTOS(NNN+2,I,J)/FLXTOS(NNN,I,J)
      ALPCLS(NNN+2,I,J)=1.0+FLXTOS(NNN,I,J)/FLXTOS(NNN+2,I,J)
   90 CONTINUE
      PRINT 99
      DO 227NNN=1,4
      DO 227I=1,3
      PRINT 228,NNN,I
  228 FORMAT(1H1,10X,4HNNN=,I2,/10X,2HI=,I2)
      PRINT 225
  225 FORMAT(10X,3HNO.,7X,10HTOTAL FLUX,5X,10HMACRO FLUX,5X,10HMICRO FLU
     1X,4X,11HSERIES FLUX,10X,5HALPHA,5X,10HCALC ALPHA)
      DO 227J=1,6
  227 PRINT 226,J,FLXTOE(NNN,I,J),FLXMAE(NNN,I,J),FLXMIE(NNN,I,J),FLXSEE
     1(NNN,I,J),ALPHAB(NNN,I),ALPCLE(NNN,I,J),FLXTOS(NNN,I,J),FLXMAS(NNN
     2,I,J),FLXMIS(NNN,I,J),FLXSES(NNN,I,J),ALPHAB(NNN,I),ALPCLS(NNN,I,J
     3)
  226 FORMAT(11X,I2,2X,6E15.5,5X,5HEXACT,/,15X,6E15.5,5X,5HSHORT)
C     SURFACE DIFFUSSION
C     WAKAO AND SMITH
      DO 92KJK=1,6
      Y1(KJK)=YA1(KJK)
      Y2(KJK)=YA2(KJK)
   92 CONTINUE
      DO 150 NNN=1,3,2
      DO 150 J=1,6
```

TABLE XXVI (Continued)

```
      AMESS=2.0*KS*DS*P(J)*(Y1(J)-Y2(J))/(R*T(J)*AL)
      FLSMAW(NNN,J)=AMESS*(EA**2)/AA
      FLSMIW(NNN,J)=AMESS*(EI**2)/AI
      FLSSEW(NNN,J)=AMESS*4.0*EA*(1.0-EA)/AA
      FLSTOW(NNN,J)=FLSMAW(NNN,J)+FLSMIW(NNN,J)+FLSSEW(NNN,J)
      Y1(J)=YB1(J)
      Y2(J)=YB2(J)
  150 CONTINUE
      DO 252NNN=1,3,2
      PRINT 99
      PRINT 253,NNN
  253 FORMAT(10X,4HNNN=,I2)
      PRINT 250
  250 FORMAT(////40X,12HSURFACE FLUX,/38X,15HWAKAO AND SMITH,//2X,3HNO.,
     110X,5HTOTAL,10X,5HMACRO,10X,5HMICRO,9X,6HSERIES)
      PRINT 251, (J,FLSTOW(NNN,J),FLSMAW(NNN,J),FLSMIW(NNN,J),FLSSEW(NNN
     1,J),J=1,6)
  251 FORMAT(6(3X,I2,4E15.4,/)///)
  252 CONTINUE
C  CALCULATION OF DAB ASSUMING AN OPEN ORIFICE
      N=6
      DELTA=AL
      ICNTOP=5
      ICNBOT=5
      DO 160NNN=1,2
      PRINT 99
      PRINT 172
  172 FORMAT(11X,3HDAB,14X,4HPDAB,13X,5HPRESS,2X,2HNO)
      DO 160NN=1,N
      TABS(NN)=T(NN)
      PMTA(NN)=P(NN)
      PCTR(NN,1,1)=YA1(NN)
      PCTR(NN,2,1)=YA2(NN)
      ANA(NN)=FLXTOE(NNN,2,NN)
      ANB(NN)=FLXTOE(NNN+2,2,NN)*(-1.0)
      PCELL(NN)=PMTA(NN)/0.0013158
C
      RRR=0.0
      JJJ=0
      GO TO (51,52,53,54,55),ICNTOP
   58 GO TO (57,59),JJJ
   57 GO TO (51,52,53,54,55),ICNBOT
C                 METHANE       CN=1
   51 PC=99.3
      VC=45.8
      TC=190.7
      BA=1.345*(TC/TABS(NN))**2
      B=-VC*(0.145-BA)
      RHO=(-1.0+(1.0+(4.0*B*PMTA(NN))/(82.05*TABS(NN)))**0.5)/(2.0*B)
      RRR=RRR+RHO
      JJJ=JJJ+1
      GO TO 58
C                   GOOF UP           CN=2
   52 PRINT173
      JJJ=JJJ+1
      GO TO 58
C                PROPANE       CN=3
   53 PC=200.0
      VC=42.0
      TC=370.0
      BA=1.345*(TC/TABS(NN))**2
      BB=0.0057*(2.0**1.5)*((TC/TABS(NN))**6)
```

TABLE XXVI (Continued)

```
      B=-VC*(0.145-BA-BB)
      RHO=(-1.0+(1.0+(4.0*B*PMTA(NN))/(82.05*TABS(NN)))**0.5)/(2.0*B)
      RRR=RRR+RHO
      JJJ=JJJ+1
      GO TO 58
C           BUTANE              CN=4
   54 PC=255.0
      VC=37.5
      TC=425.2
      BA=1.345*(TC/TABS(NN))**2
      BB=0.0057*(3.0**1.5)*((TC/TABS(NN))**6)
      RHO=(-1.0+(1.0+(4.0*B*PMTA(NN))/(82.05*TABS(NN)))**0.5)/(2.0*B)
      RRR=RRR+RHO
      JJJ=JJJ+1
      GO TO 58
C          HELIUM OR NITROGEN     CN=5
   55 RHO=PMTA(NN)/(82.05*TABS(NN))
      RRR=RRR+RHO
      JJJ=JJJ+1
      GO TO 58
C
   59 TOTN=ANA(NN)-ANB(NN)
      RHO=RRR/2.0
      C1=PCTR(NN,1,1)-ANA(NN)/TOTN
      DABT=TOTN*DELTA/RHO
      DABB=ALOG((PCTR(NN,2,1)-(ANA(NN)/TOTN))/C1)
      DBA(NN)=DABT/DABB
      PDAB(NN)=DBA(NN)*PCELL(NN)
      PRINT 171,DBA(NN),PDAB(NN),PCELL(NN),NN
      PDAB(NN)=DBA(NN)*P(NN)
      PRINT 174,DBA(NN),PDAB(NN),P(NN),NN
  160 CONTINUE
  171 FORMAT(1X,3(E15.10,2X),I2,5X,17HPRESSURE IN MM HG)
  173 FORMAT(1X,7HGOOF UP)
  174 FORMAT(1X,3(E15.10,2X),I2,5X,17HPRESSURE IN ATMS.,//)
      GO TO300
      END
```

TABLE XXVII

PELLET DATA

Columbia Carbon NXC Activated Carbon

ρ Block	0.722
E_a ($r > 150$ Å)	0.2182
E_i ($r < 150$ Å)	0.5790
$\overline{r}_a$	8936.0 Å
$\overline{r}_i$	5.79 Å
S	1200 m^2/g

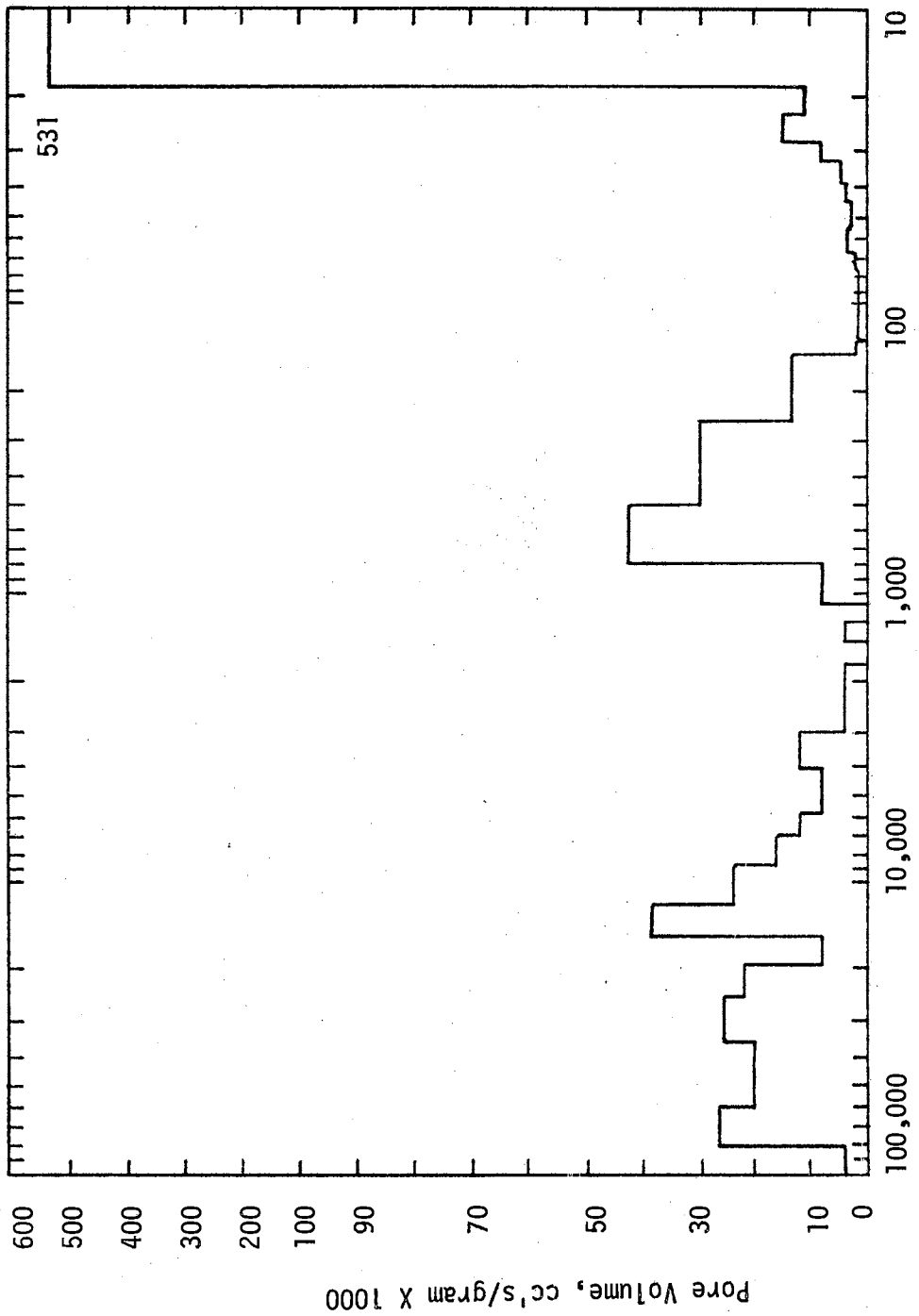

Figure 10. Pore Size Distribution -- Columbia Carbon NXC Activated Carbon

NOMENCLATURE

L = Length
M = Mass
m = Moles
P = Pressure
T = Temperature
t = Time

Symbol	Quantity	Dimensions
A_m	Constant in Langmuir Adsorption Isotherm	$/\overline{m}/L^{2}/$
b	Constant in Langmuir Adsorption Isotherm	$/\overline{T}/P/$
C	Molar Gas Density	$/\overline{m}/L^{3}/$
$\overline{C}$	Molar Adsorbate Density	$/\overline{m}/M/$
$\overline{C}'$	Molar Adsorbate Density	$/\overline{m}/L^{2}/$
C_m	Coefficients in Equation (22)	
C_n	Coefficient in Equation (23)	
C_R	Coefficient in Equation (29)	
D	Diffusivity	$/\overline{L}^{2}/t/$
E	Porosity	
H	Henry's Law Constant	$/\overline{m}/MP/$
K'	Coefficient in Equation (44)	
K_o	Coefficient in Equation (3)	
K(P)	Factor in Equation (32)	$/\overline{m}/MP/$
K_S	H·R·T	$/\overline{m}/MP/$
K	Tortuosity Factor	
L	Length or Distance	$/\overline{L}/$
M	Molecular Weight	$/\overline{M}/m/$
N	Molar Flux	$/\overline{m}/tL^{2}/$

Symbol	Quantity	Dimensions
P	Pressure	$[P]$
p	Partial Pressure	$[p]$
q	Tortuosity Factor	
R	Ideal Gas Law Constant	$[PL^3/mT]$
r	Radius	$[L]$
S	Specific Surface Area	$[L^2/M]$
T	Temperature	$[T]$
u	Velocity Component in Equations (22) and (23)	$[L/T]$
v	Molecular Velocity	$[L/t]$
W	Gas Flow Rate	$[m/t]$
X	Mole Fraction	
Z	Gas Compressibility	

Greek Letters

α	As Defined in Equation (7)	
∂	Partial Derivative	
λ	Molecular Mean Free Path	$[L]$
μ	Viscosity	$[M/Lt]$
π	3.1416	
ρ	Mass Density	$[M/L^3]$
Σ	Summation	
τ	Time Between Molecular Movements on Surface	$[t]$
ϕ	Spreading Pressure	$[P]$

Subscripts

Symbol	Quantity
A	Component A
a	Macropores
B	Component B
D	Bulk Gaseous Diffusion
E	Effective
EFF	Effective
i	Micropores
K	Knudsen Diffusion
L	At Pellet Face L
O	At Pellet Face O
S	Surface Diffusion

VITA

Thomas J. Kelly

Candidate for the Degree of

Master of Science

Thesis: GASEOUS AND SURFACE DIFFUSION IN ACTIVATED CARBON

Major Field: Chemical Engineering

Biographical:

Personal Data: Born in Oklahoma City, Oklahoma, the son of Mr. and Mrs. James J. Kelly.

Education: Graduated from St. Gregory's High School, Shawnee, Oklahoma, in 1961; received the Bachelor of Science degree from the University of Notre Dame in 1966, with a major in Chemical Engineering; completed requirements for the Master of Science degree at Oklahoma State University in May, 1968.

Professional Experience: Chemical Engineer Trainee, Kerr-McGee Corporation, Summer 1963 and Summer 1966.